Statement of originality of the MSc thesis

I declare that:

1. this is an original report, which is entirely my own work,

2. where I have made use of the ideas of other writers, I have acknowledged the source in all instances,

3. where I have used any diagram or visuals I have acknowledged the source in all instances,

4. this report has not and will not be submitted elsewhere for academic assessment in any other academic course.

Student data:

Name: Guus Cals

Registration number: 3939189

Date: 09-08-2017

Signature: 

Grain fracturing and grain re-arrangement in sands and sandstone: Studying brittle deformation features in sugar glass as an analogue.

Cals, G.P.H., Hangx, S. J. T., Peach, C.J., Schimmel, M.T.W.

Abstract

In order to better understand the effect of extracting or injecting fluids can have on a sandstone reservoir, the knowledge on the mechanical behaviour should be improved. This study focusses on this aspect by using sugar glass as an analogue for quartz sand. This is done by performing experiments on a hexagonal and cubic packs of sugar glass discs, with or without flattened contact areas. The results were then compared to micrographs from experiments on sand aggregates in order to determine whether sugar glass is a good analogue for quartz sand.

Aggregates build out of discs of sugar glass were deformed using an Instron 8862, which compressed the different samples in a vertical direction. This compaction caused the failure of multiple discs. The cracks formed in these failed discs were subdivided into different categories: meridional, straight, convergent, and spalling cracks. In the experiments on cubic packing, the majority of cracks formed in a vertical direction. In the rotated cubic and hexagonal experiments, the majority of cracks formed at an oblique angle.

The packing of the aggregates caused a big difference in structures that formed in the aggregate. These structures could be compared to micrographs of sand aggregates. The structures formed in the hexagonal experiments were more similar than the structures formed in the cubic experiments. In the sand aggregates, most cracks recognizable in the quartz sand grains were at an oblique angle to the compaction direction. Also the type of cracks was very similar: a multitude of contact-to-contact meridional and convergent cracks.

Another important feature arises in the rotated cubic experiments with flattened contacts: due to slip along the boundaries of the discs, cracks formed in a standard pattern. The cracks that form due to this grain boundary slip all form on the edges of the contact area and break off a side of the disc. These patterns can be used to predict structures in deforming sandstones or sand aggregates and to improve models on sandstone reservoir behaviour.

1. Introduction

Subsurface sandstone reservoirs can have a relatively high porosity (up to 25-35%, Ehrenberg and Nadeau, 2005), meaning they can serve as a store for different fluids, such as hydrocarbons, water/brine or CO_2. When these fluids are extracted, the pore fluid pressure in the reservoir decreases while the overburden stress remains constant, leading to an increase in the effective stress on the sand grains. This can cause both elastic and inelastic deformation, leading to reservoir compaction and/or subsidence of the surface (causing disturbance in the flow patterns of the rivers or a relative rise of the sea level) or production problems (reduction of permeability, well instability). In a strongly fractured reservoir like the Groningen Gas Field, differential compaction may lead to induced microseismicity. Therefore, understanding the mechanical behaviour of sandstone under compression is key.

Inelastic deformation in sand grains under upper crustal, low temperature conditions is mainly controlled by brittle grain failure driven by grain-contact-stress, accompanied by grain rearrangement. A theory has been developed to describe the stress distribution in grains. This so-called Herzian contact theory (e.g. Hertz, 1881) describes the stress distribution between two grains through analytical equations. A problem with this theory is that it works for single, frictionless contacts. However, in sandstones grain contacts do not consist of points, but of irregular planes (sutured or indented contacts). This means that the stress along the contact is hard to calculate analytically. The cracks that emanate from an indented or sutured contact plane might form at higher stresses than those required to induce cracking at contact points. Grain failure will lead to grain-scale strain, by grain crushing and re-arrangement of the fragments. The development of grain strain,

from grain failure, and grain contact stress for different packing configurations cannot be easily measured for sand grains, and is usually approached using transparent and/or photo-elastic materials (see Hiramatsu and Oka, 1966). However, it is possible to use analogue materials such as transparent sugar glass and photo-elastic Plexiglas. Since the development of fracturing is relatively hard to study, very few see-through experiments have been conducted

In this research, I will study the effects of flattened contact surfaces on the formation of fractures in disc-shaped 'grains', as an analogue to sand grain deformation in a sandstone. This research will expand on the study done by Dik et al. (2016), who performed see-through experiments on circular sugar glass discs, having contact points instead of contact planes. For this study I will be using the same setup, but using different grain sizes and grain shapes.

Aims and Objectives

- Describing how brittle deformation occurs in regular packs of sugar glass discs with and without flattened contacts
- Describing the effects of a different packing of the discs (hexagonal, cubic or 45^{o} rotated cubic) on the type of cracks that form in failed sugar glass discs
- Comparing the results of the analogue model (sugar glass disc experiments) with microstructures showing the deformation of real sand grains, to see whether the analogue model is representative for the deformation of real sand grains

2. Methods

2.1 Sample and pore fluid preparation

The experiments were performed on sugar glass discs. The sugar glass, or isomalt, consists of 50% glucose, 25% sorbitol and 25% mannitol. The isomalt was heated to 170 °C in a glass beaker in order to melt it This was done with an RCT Basic electronic heating plate, which was coupled to a thermometer in order to measure the temperature of the isomalt. After the isomalt was molten, it was poured into a Teflon mould. For the first experiments (done on circular discs) the mould consisted of 30 circular slots with a thickness of 4.5 mm and 10-mm diameter. When filling the slots, a small head forms on top of the disc which contains some air bubbles. After filling these slots, the isomalt was left in the salt preparation room (18 °C and low (<20%) humidity) to cool and harden. A disadvantage of this method was that all of the slots were of slightly different sizes, making it more difficult to later achieve a perfect packing. After hardening, the discs were sanded with a size 400 sandpaper to which water was added in order to accelerate the process. Hereafter, the discs were pushed out of the mould into a bath of methanol, in order to remove all of the water, preventing the discs from dissolving. However, this formed a small layer of milky-white substrate on the surface of the discs, resulting into an opaque surface. This was later sanded off again using dry sand paper (size 400) and a small mould which was made to the final thickness of the discs (4.0 mm). The edges of the sugar glass discs were sanded with a 1000 sized sandpaper in order to clean them to fit in rows in the experimental cell. Half discs were made by cutting a disc in two, usually resulting in one broken half and one intact half. However, since this was not done with a mould, the size of the half discs could vary, causing difficulties in packing of the discs.

In order to create flattened sides for the cubic setup, a third mould was created, which made it possible to file off sides of the discs. During these steps, the discs were touched with silicone gloves to minimize the contact of the discs with any water. After preparation of the discs, they were stored in open beakers in the low-humidity salt preparation room.

As a pore fluid silicone oil was used which was coloured blue using Oil Blue A colouring. Before adding the oil to the experimental setup, it was heated to 140 °C, in order to remove trace amounts of water that might be present in the oil. After the oil cooled down, it was stored in a sealed plastic beaker.

2.2 Experimental setup

The sugar glass discs were placed in a steel experimental cell with two glass walls. Before the discs were placed inside the cell, a small amount of blue oil was placed at the bottom of the cell. This was done to prevent air bubbles

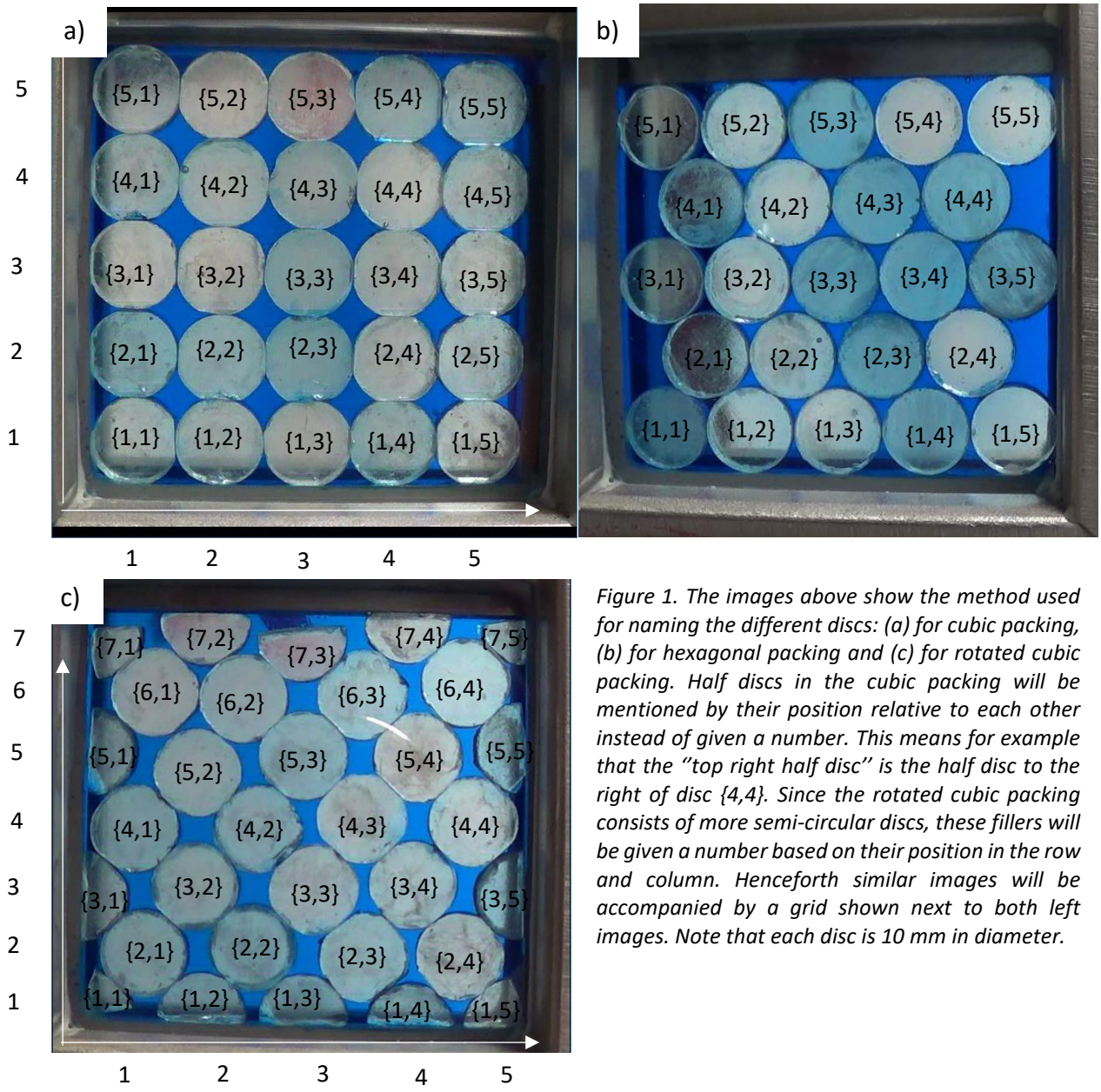

Figure 1. The images above show the method used for naming the different discs: (a) for cubic packing, (b) for hexagonal packing and (c) for rotated cubic packing. Half discs in the cubic packing will be mentioned by their position relative to each other instead of given a number. This means for example that the "top right half disc" is the half disc to the right of disc {4,4}. Since the rotated cubic packing consists of more semi-circular discs, these fillers will be given a number based on their position in the row and column. Henceforth similar images will be accompanied by a grid shown next to both left images. Note that each disc is 10 mm in diameter.

to remain between the pores. Hereafter, the discs were placed in layers above each other. This was done in three different configurations, using simple cubic packing, a 45° rotated cubic packing or simple hexagonal packing (Figure 1). Due to the small differences in disc size mentioned earlier, some rows in the hexagonal and rotated cubic experiments were slightly too wide, causing stacking difficulties and making it difficult to reproduce the same packing every time.

After this preparation, the experimental cell was placed inside an Instron 8862, which was used to load the cell. The Instron was equipped with a 10 kN load cell. A camera was attached to the frame of the Instron in order to visually monitor the deformation of the discs. A blank sheet of paper was placed behind the camera and behind the experimental cell to minimize the effect of colour distortion and reflections on the glass and thus resulting into a clearer image. A picture of the final setup can be seen in Figure 2. Hereafter the Instron was set up to compress the sample with a displacement rate of 3.6 mm/h. The pore fluid was able to escape along the sides of the discs and along the piston, resulting in an atmospheric pore fluid pressure. The surrounding temperature was kept at room temperature (~21 °C).

Figure 2. A picture of the experimental setup. The experimental cell is placed in the frame of the Instron and the sample is compressed by the upwards movement of the base of the machine.

2.3 Data logging and processing

The videos of the experiment were converted to MPEG files using Freemake Video Converter, in order to open them in the video editor program VirtualDub. This program was used to study the videos frame by frame and accelerate the videos of the experiments to create ones of around 6 minutes. Per set of experiments one sped up video was put online (see Appendix). Apart from the videos recorded during the experiments the Instron position, temperature, and Instron load were measured as well. These data were placed in Excel files so that stress-strain diagrams could be constructed.

2.4 Nomenclature of fractures

In order to describe the cracks forming in the different discs, the sugar glass discs will be numbered as followed: {row nr., column nr.}, starting at the bottom left with disc {1,1} (see Figure 1). In the hexagonal packing, semi-circular discs will be mentioned by their position relative to each other instead of given a disc number. This means for example that the ''top right half disc'' is the semi-circular filler disc to the right of disc {4,4}. Since the rotated cubic packing consists of much more semi-circular discs, these fillers will be given a number based on their position in the row and column. This is also shown in Figure 1.

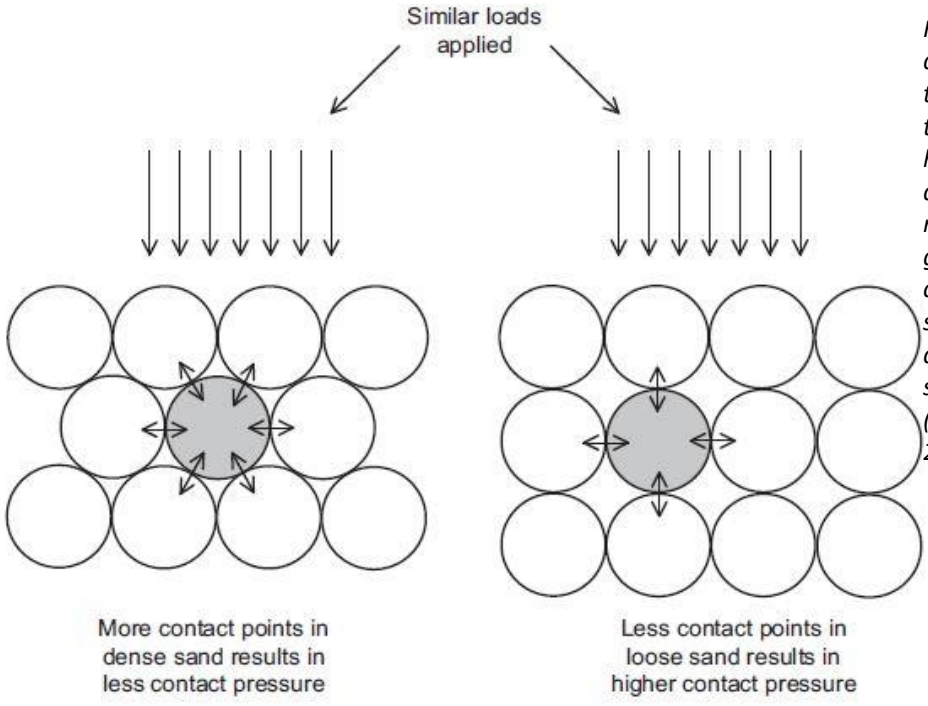

Figure 3. The stress distribution according to the Herzian contact theory for cubic and hexagonal packing is dependent on the number of contacts a grain has: the more contacts, the lower the stress at the contacts and thus the overall stress in the aggregate. (After Omidvar et al, 2012)

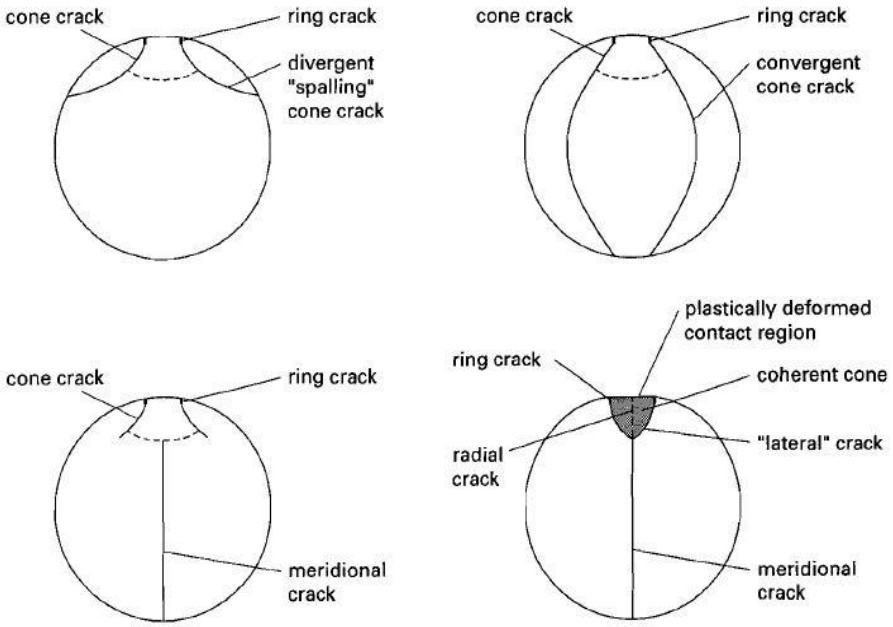

Figure 4. Different types of cracks that can form in compressed spheres (Brzesowsky, 1995, Figure 2.13). These names will be used to describe the cracks formed in the sugar-glass discs with a cubic packing.

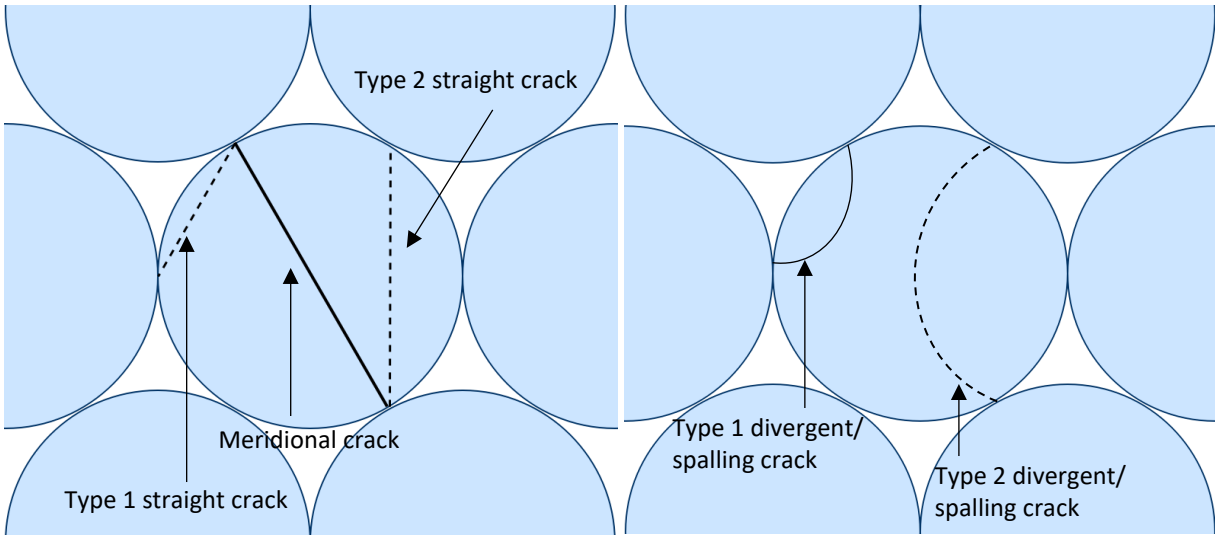

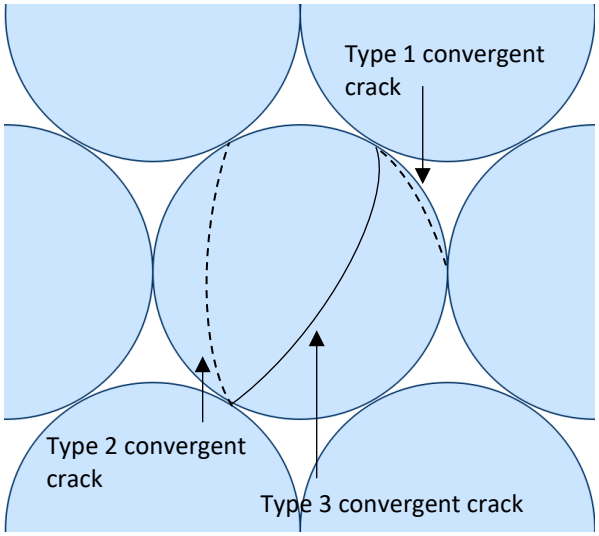

Figure 5. Different types of cracks that can form in a hexagonal packed system: in a) three types of straight cracks are shown, in b) two types of divergent cracks, and in c) three types of convergent cracks. These names will be used in the description of the cracks.

Failure of the discs is caused by the stress-distribution in the discs. The more contact points a disc has, the lower the stress at the contacts (Omidvar et al., 2012, see Figure 3) and thus the lower the overall stress throughout the disc. Since cracks form between two places with high stress, most cracks will form between the contact surfaces. However, some cracks can form between two contacts, since the tensile stress at the contact area is highest but still remains (although decreased) outside these contact areas (Brzesowski et al., 2011). Since the packing of the grains (cubic or hexagonal) controls the number of contact points and their position - and thus the symmetry of the formed cracks -, the description of the cracks will be different for the hexagonal and the cubic packing packings.

2.4.1 Nomenclature of fractures in a cubic packing

Brzesowsky (1995) showed that cracks that form in diametrically-loaded spheres can be described by the configurations they form in (see Figure 4). One type of fractures that can form in sand grains are ring cracks. At low compression rate (≤ 0.1 mm/min) they are formed in a divergent shape (spalling cracks), while at higher compression rates (≥ 0.5 mm/min) the ring cracks form in a convergent shape (union peel cracks). Another type of possible fractures are meridional cracks. They split the grains in half and crack along a straight path (along the meridian). At the contact surface grains can get flattened by plastic deformation or crushing due to high strain.

These same type of cracks can be identified in failed sand grains, and thus will also be used in this research to describe the cracks formed in the sugar glass discs. Since the spheres on which the experiments were performed were compressed diametrically with two contact areas (one on the top and one on the bottom), the packing is found to conform to the cubic packing, and thus will be used to describe the structures that formed in said packing.

2.4.2 Nomenclature of fractures in hexagonal packing.

Since in a hexagonal packed aggregate the discs to have six contacts with neighbouring discs, the cracks can form in many more different orientations. The nomenclature of these different cracks can be seen in Figure 5.

The straight cracks that go across the whole disc are called meridional cracks. Meridional cracks split the disc in two equal parts. Other straight cracks are named differently, since they do not form along the meridian. The ‘’type 1 straight cracks’’ form between two neighbouring contacts, the ‘’type 2 straight cracks’’ form between a contact and the second closest contact. ‘’Type 1 spalling (or divergent) cracks’’ form between a contact and the neighbouring contact as well, but their path diverges from the meridian. ‘’Type 2 spalling cracks’’ have the same divergent path, but they form between a contact and the second closest contact. ‘’Type 1 convergent ring cracks’’ form between a contact and its closest contact. A ‘’type 2 convergent ring crack’’ forms between a contact and its second closest contact and a ‘’type 3 convergent ring crack’’ forms between a contact and the contact opposite of it.

3. Results

3.1 Sugar glass experiments on circular discs

In order to see whether the conditions of the recent experiments are comparable to the ones during the experiments of Dik et al. (2016), first an experiment was performed on three layers of hexagonally packed, circular sugar glass discs. The results of this experiment were similar to the results obtained by Dik et al. The biggest difference between this experiment and the ones performed by Dik et al. was the fact that it took longer for the first cracks to form (23 minutes instead of 16) and a higher load was necessary in order to form these first cracks (-2.0 kN instead of -0.76 kN). However, in the three experiments performed by Dik et al., the time in which the first cracks form varies between 9 minutes and 16 minutes, and the load needed to form the first crack varies between -0.42 and -0.98 kN. This indicates that there is a relatively high variability on when the first discs will break.

Below, the results of the different experiments will be discussed. A more detailed description of the failure of the discs can be found in the Appendix, accompanied by

pictures of the experiments and links to sped up films of the experiments.

3.1.1. Hexagonal packing, no semi-circular filler disc

3.1.1a. Stress-strain development

In Figure 6a, the stress-strain diagram is shown for a 5-layered simple hexagonal packing without the use of semi-circular discs to fill the empty slots on the sides. In Table 1 the details of the different experiments can be found. What can be seen in the experiments is that the formation of a crack causes a drop in the load, which translates to a drop in stress. The first cracks form around 1.5 kN, or 7.5 MPa. This becomes visible in both the stress-strain diagrams, where the first stress drop can be seen at around 7.5 MPa, and in the movies of the experiments, from which bar charts were constructed showing the number of discs that are cracked in a certain stress or strain interval (Figures 7a and 8a). After the formation of these first cracks, the load is relatively quickly restored to the value before failure. In experiments H5L3 and H5L4 this trend of stress drops followed by quick recovery occurs until a strain is reached of 7.85%. Here, multiple discs fail at the same time, causing a big stress drop. After this failure event, other discs fail at stress-levels that were already reached at lower strain. At a lower compaction rate (experiment H5L1), the load at which the first discs fail is higher (in this case 12.0 MPa). The only big fracture event in experiments H5L1 takes place at the same stress value as the big events mentioned before in experiments H5L3 and H5L4.

Near the end of every experiment, the variation in stress has increased immensely compared to the variation visible at the start of the experiments (see Figure 6a and 9b). This increase in variation cannot be explained by the background noise, since the amplitude of the background noise is much smaller and the wavelength is larger. Also the small variations near the end of the experiments occur with more regularity than the background noise (see Figure 9a).

3.1.1b. Description of deformation in the discs

The first deformation that takes place in the discs can be seen as flattening of the discs at the contacts. This flattening can be seen in every disc at every contact. This suggests that the stress is evenly distributed throughout the whole packing, but is focussed at the contacts. The first discs to show major failure are the ones at the top or the bottom row (see Figure 10a), where the sugar glass discs are in contact with the steel. The cracks that accompany this failure form between two contact surfaces and are usually type 2 non-curved cracks, forming V- or Λ-like structures within the discs (see Figure 10b). Another feature is that multiple parallel meridional fractures can form at the same time or at different times between the same two contacts. These meridional cracks can be accompanied by an array of ''type 3 convergent cracks'' that form between these same contact surfaces, as can be seen in Figure 10a in disc {5,5}, and form at the same time as the meridional cracks. If there is space left in the row, the disc is pushed open horizontally along these cracks. The contact areas where these cracks have formed between are heavily deformed as well. These contacts consist of multiple microcracks that spread out in many different directions. At a later stage type 1 and 2 divergent cracks form from these microcracks at this crushed contacts.

The discs in the middle three rows - the ones without a sugar glass to steel contact and thus the ones with the least effect of the steel boundary- show less deformation. Less discs have failed and the failed discs show less fractures. However, the failed discs still show similar cracking patterns to the discs on the top and bottom rows: the cracks run from one contact to another, the first cracks to form are meridional cracks and are accompanied by ''type 3 convergent cracks'', and the fractures form in a near-vertical direction. Microcracks can behave differently: these cracks can form from one surface to the centre of the disc, can form in the centre of the disc without touching any contacts or form in multiple directions.

3.1.1c Initiation of cracks

The position where the cracks form can provide vital information about the stress distribution in the sugar glass discs and about the crack patterns that form in quartz grains. The main focus will be on the central seven discs (highlighted in Figure 12), since these discs are

a)

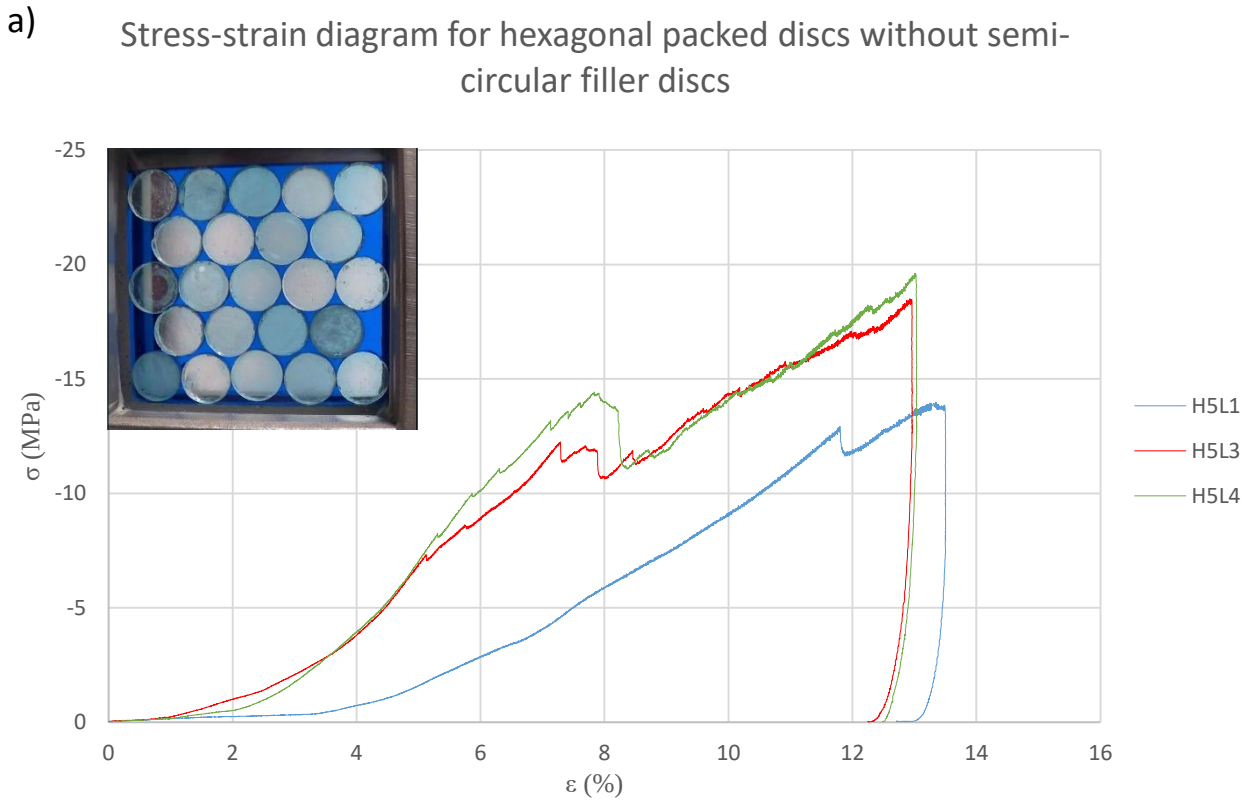

b)

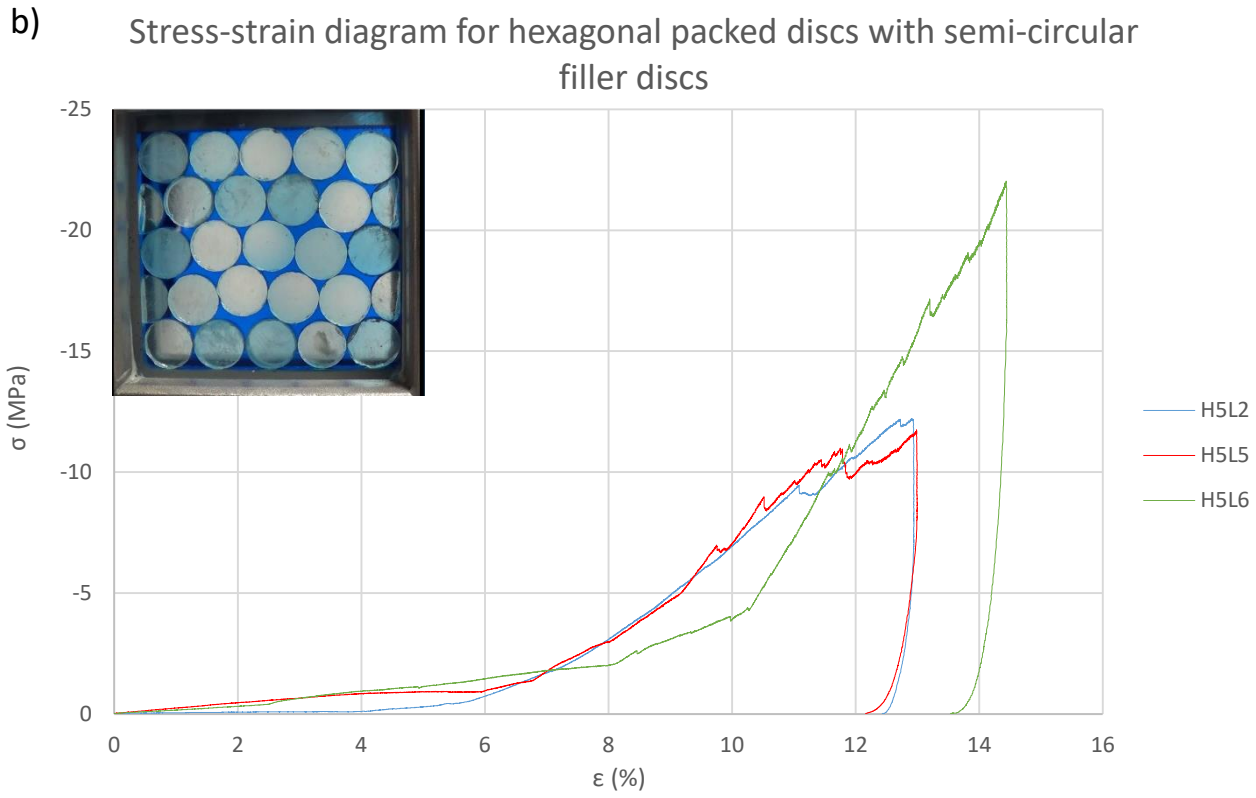

Figure 6. Stress-strain diagrams for experiments performed on hexagonal packed discs without (a) or with (b) semi-circular filler discs. σ is shown negative since the compression direction was measured as negative.

a)

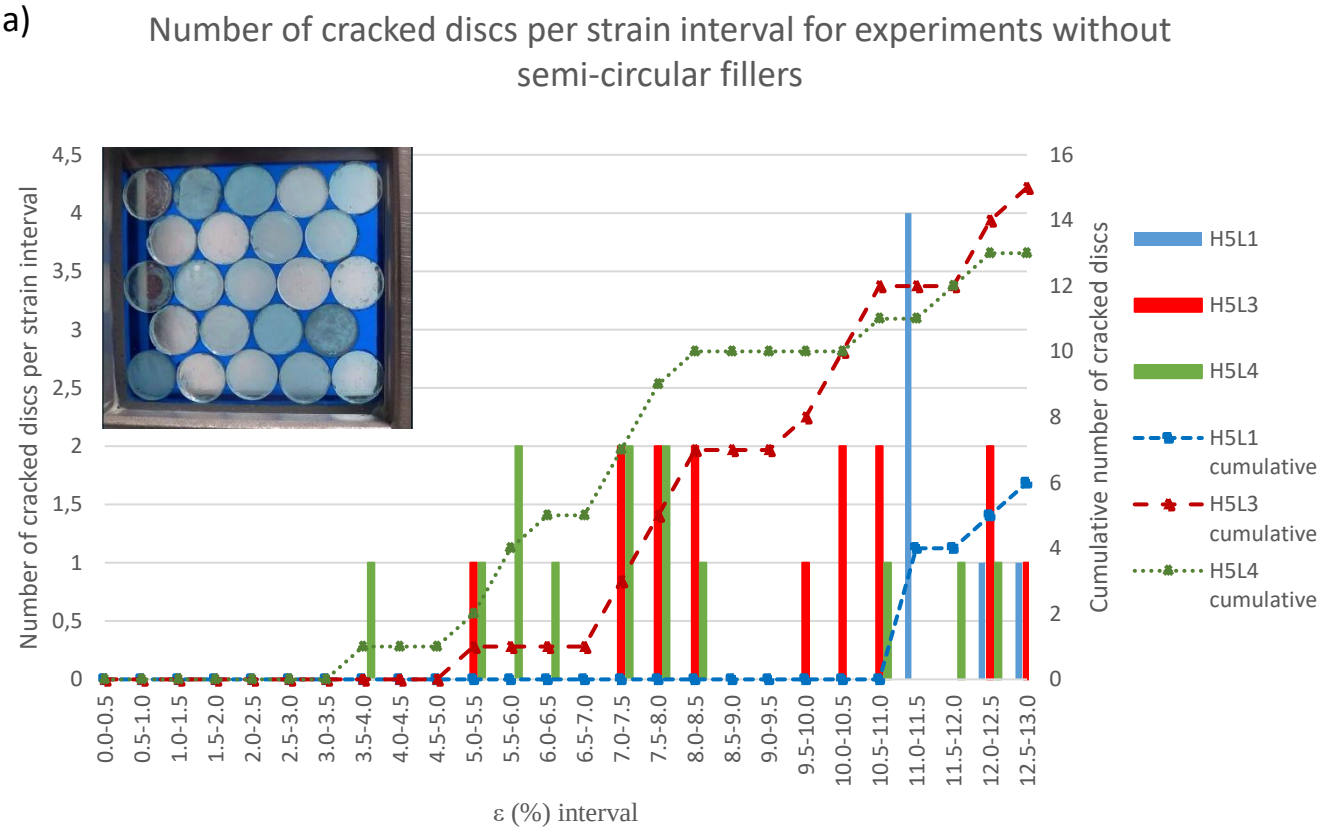

b)

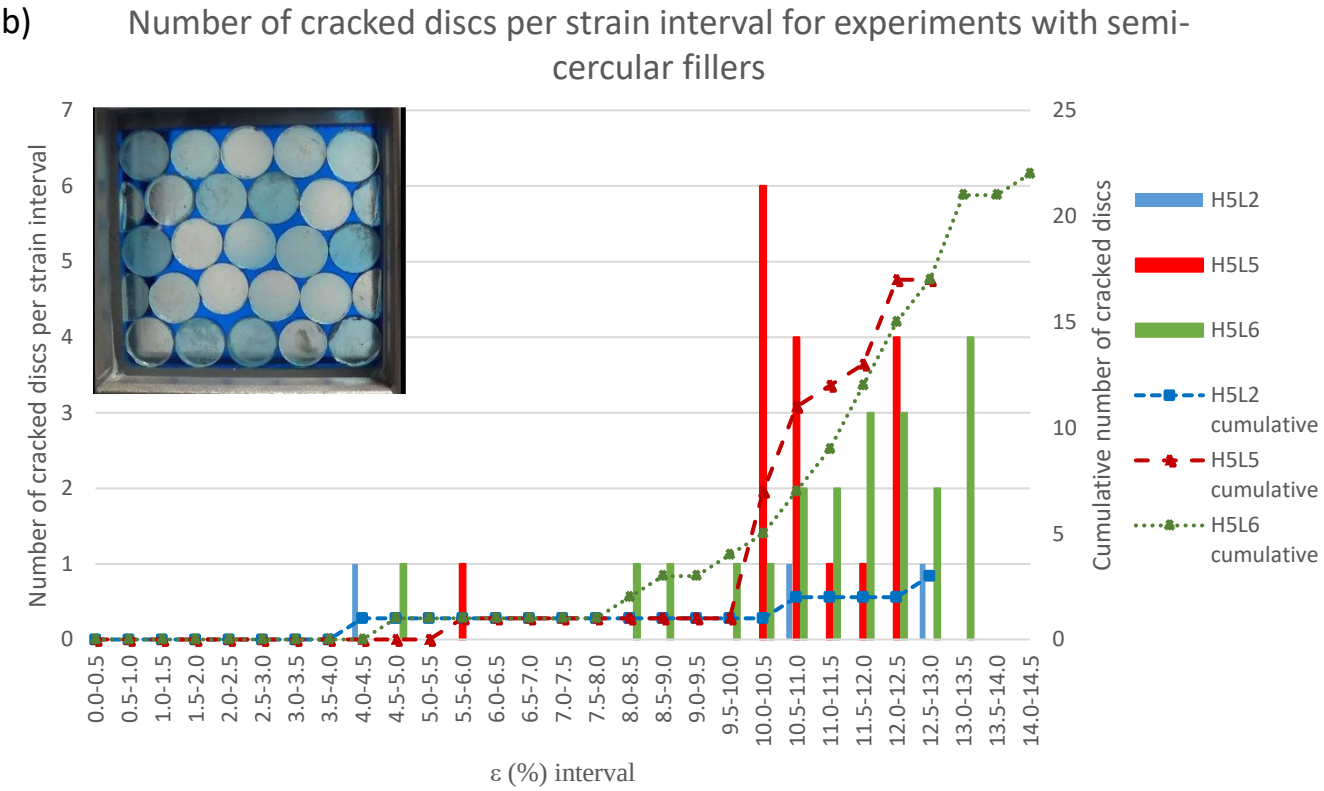

Figure 7. The amount of cracked discs per strain interval for experiments without (a) and with (b) semi-circular filler discs. In experiments without the filler discs, the discs appear to fail independently of strain, since no big increases in crack formation can be recognized. In the experiments with filler discs, horizontal cracks form first (the three bars between 4.0 and 6.0 % strain), later followed by the formation of vertical cracks. These vertical cracks form in bigger events, where multiple discs fail at the same time, resulting in a larger number of cracks in a certain strain interval.

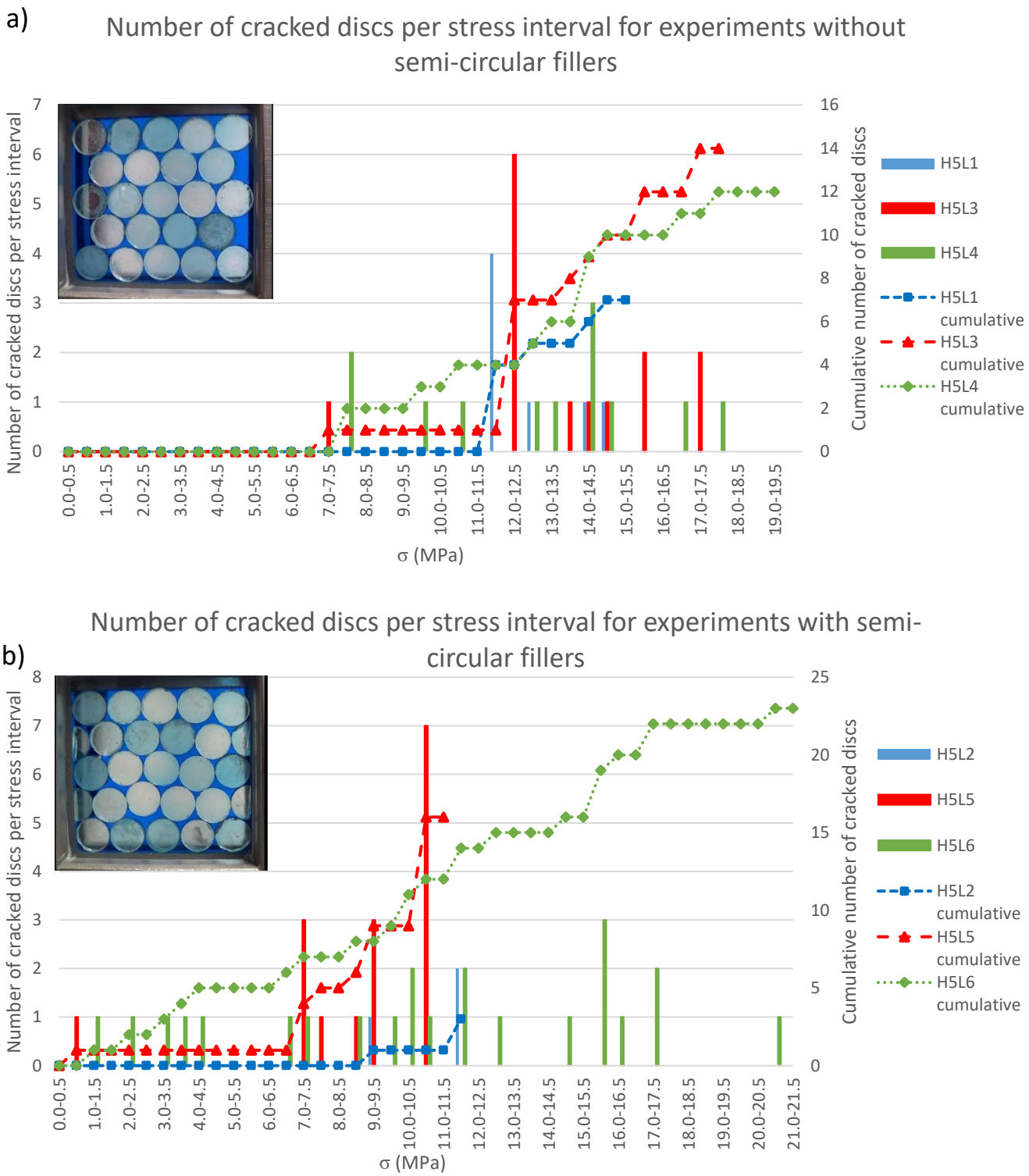

Figure 8. The amount of cracked discs per stress interval for experiments without (a) and with (b) semi-circular filler discs. In these Figures compressive stress has been take positive. a) In experiments without the filler discs the first discs start to fracture at 7.5 MPa, while most of the cracks form between 11.0 and 18.0 MPa. b) In experiments with the semi-circular fillers, the first discs crack at 1.0 MPa. These cracks are horizontal cracks caused by the limitations the filler discs cause on the horizontal expansion of the discs and thus increasing the horizontal stresses. The majority of the cracks form between 7.0 and 12.0MPa, which is lower than the stress that caused fracture in the experiments without filler discs.

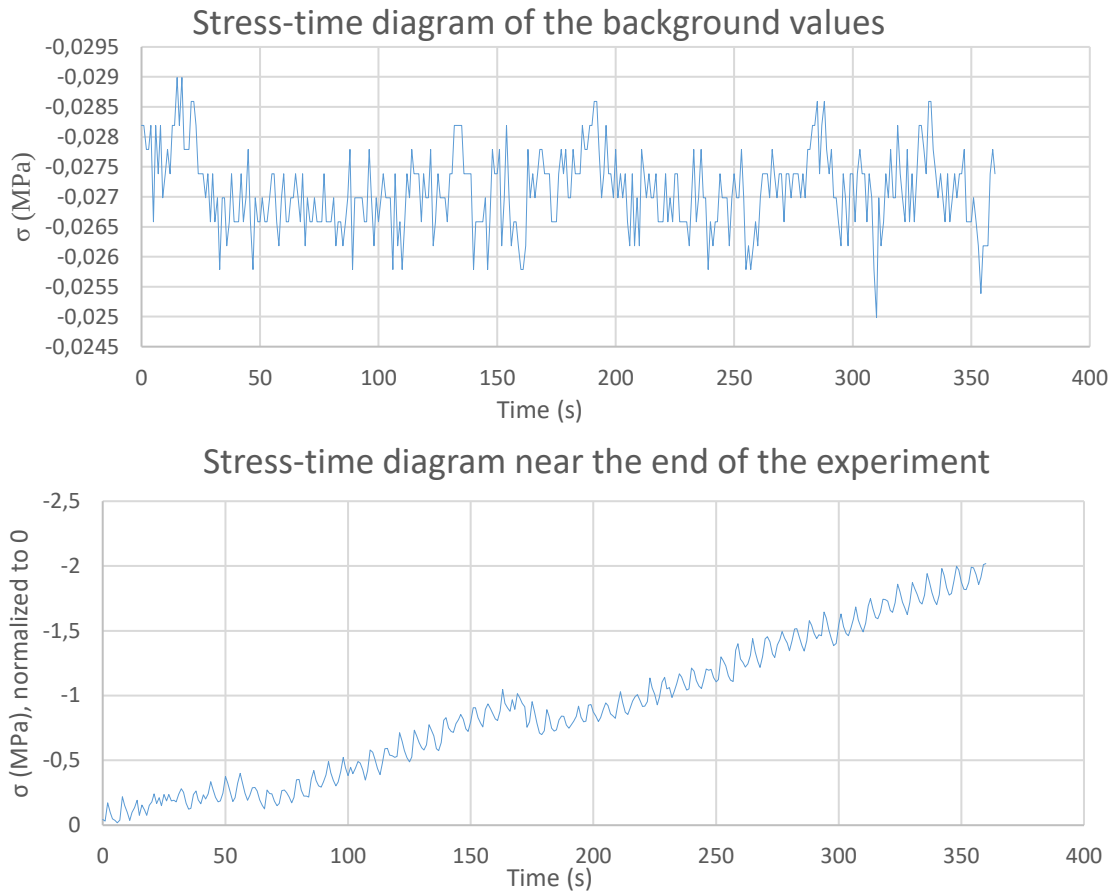

Figure 9. a) The variations in stress caused by background variation. Note that the stress difference caused by the background is very low. The wavelength of the background signal is very irregular. b) This figure shows that the variations in load near the end of the experiments (in this case H5L4) are of a much bigger scale than the variations in the background. The mean wavelength of these variations is different: the mean wavelength in the background is roughly 44 s, while the wavelength of the variation near the end of the experiment is 6 s. Furthermore, the variations near the end of the experiment occur with a higher regularity than the background signal. In both diagrams compressional stress is taken as negative.

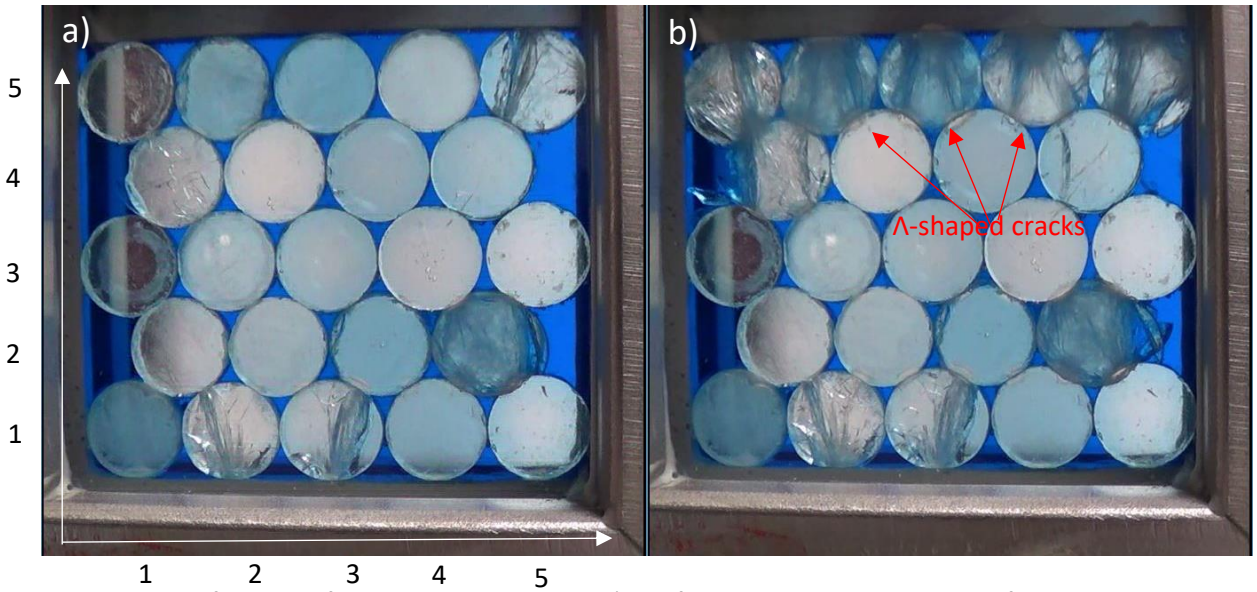

Figure 10. Deformation features in sample H5L4. a) The first discs to show the most deformation are usually at the top and bottom row. b) At a later stage, more discs in the centre have failed, while the top row completely failed. The cracks in this row are mostly Λ-shaped. Disc {2,4} has been deformed intensively and pieces have been broken off that moved into the open space. The same can be seen in discs {4,1} and {5,5}.

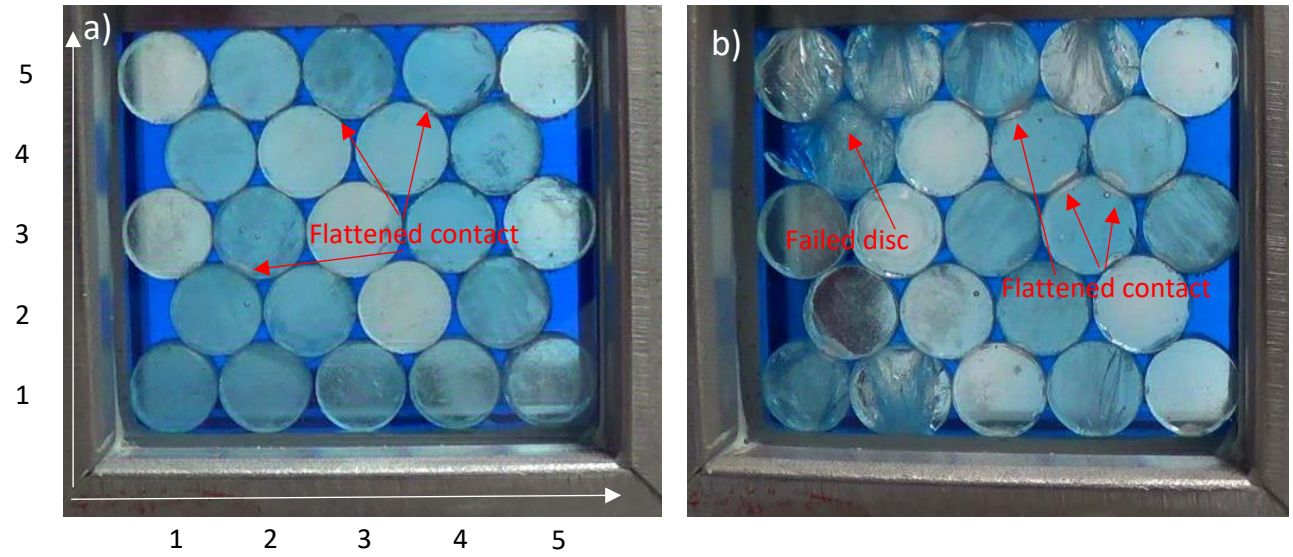

Figure 11. The deformation at a strain of 10.5% for experiments H5L1 (a) and H5L3 (b). Note that the deformation in (a) took place only at the contacts, which have flattened, while the deformation in (b) resulted in both flattening and failure of discs.

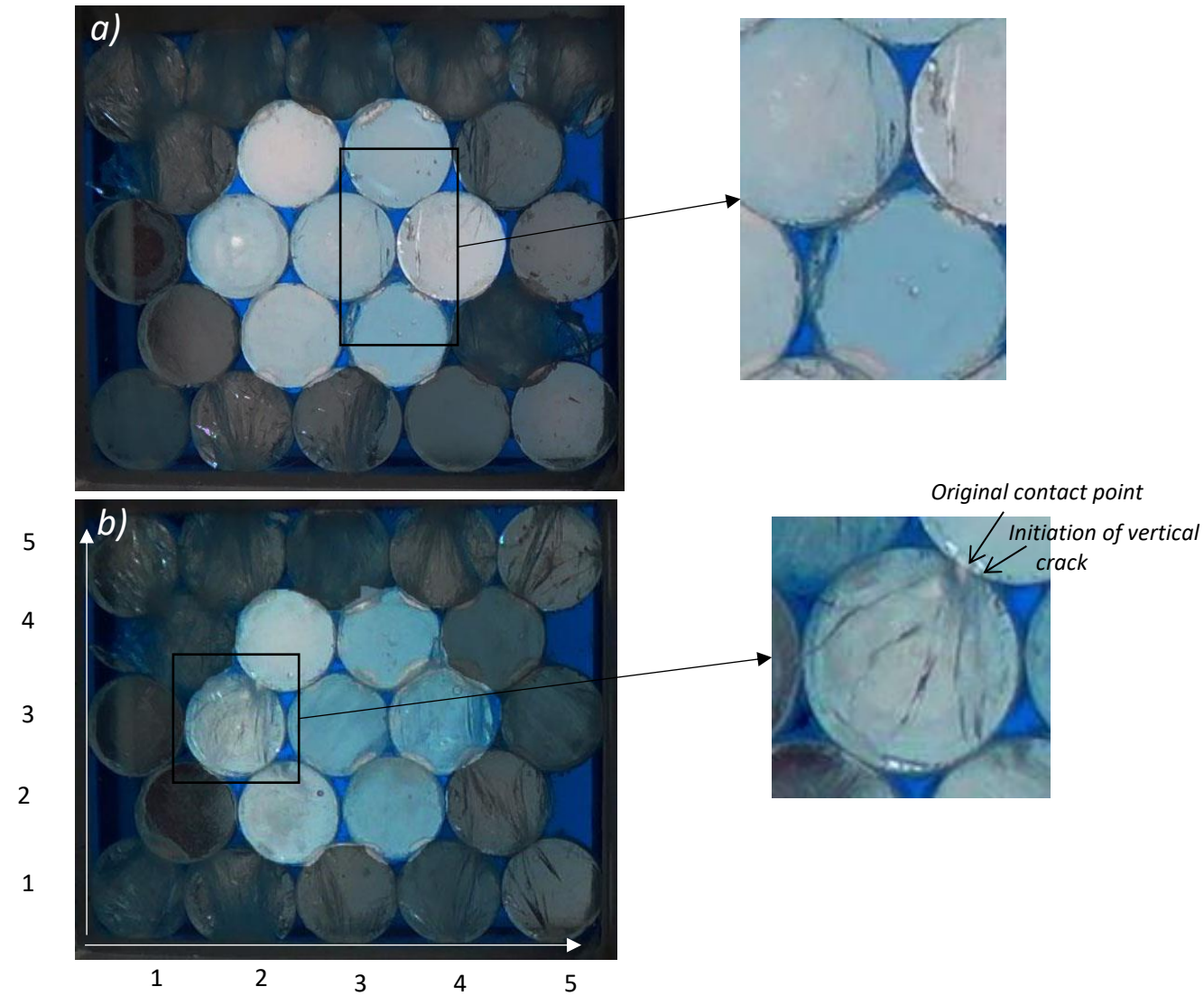

Figure 12 The places where cracks initiate at the edges of the discs in a hexagonal packed system. The cracks form just outside the contact point instead of direct at these points. (a) for experiment H5L4, (b) for experiment H5L3.

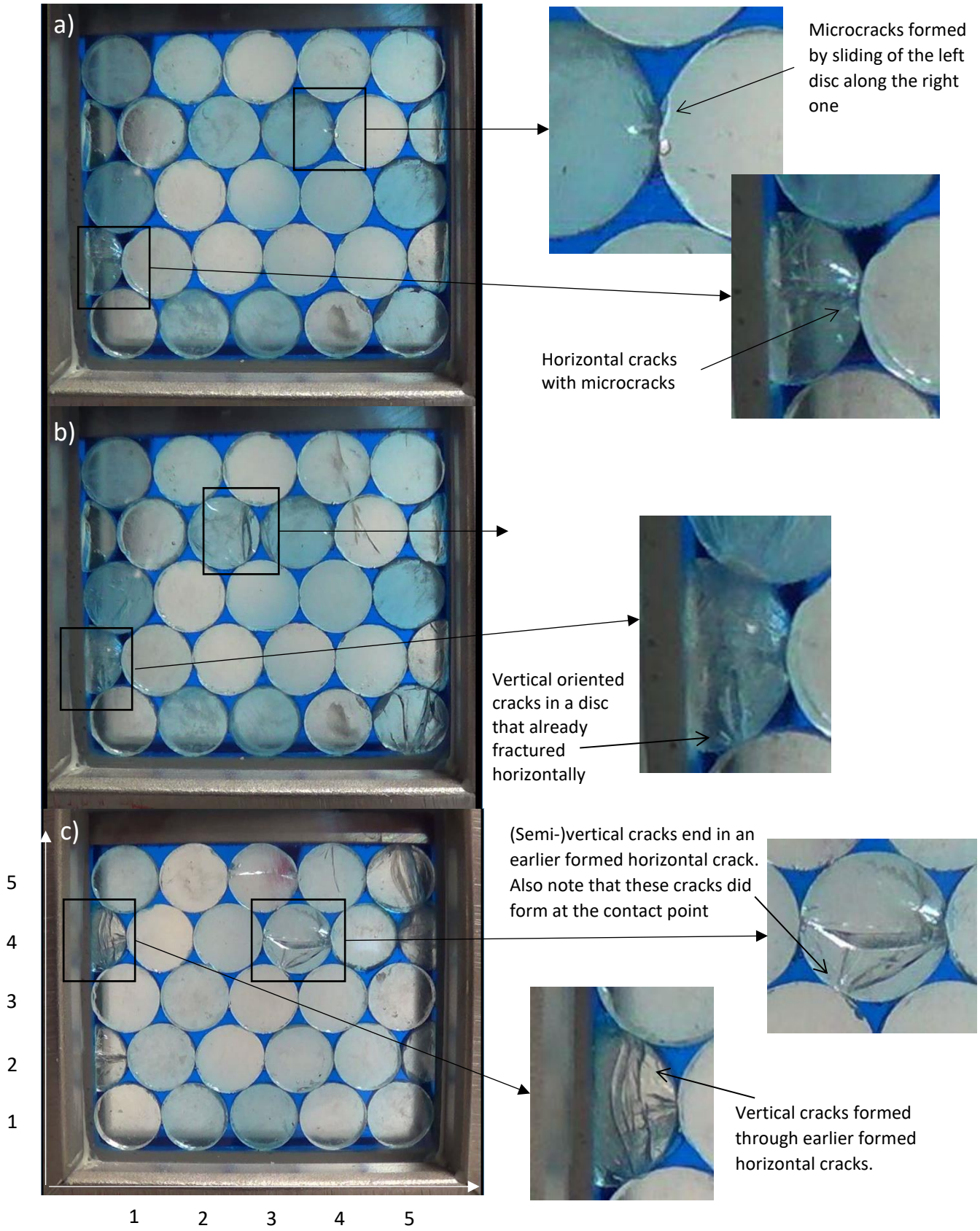

Figure 13. a) In experiment H5L5 microcracks can be seen that have been formed by the movement of the discs into the open spaces. In the bottom left semi-circular filler disc, meridional cracks have formed with the presence of multiple microcracks. b) At higher stress, vertical cracks start forming in the discs. These cracks can run through already existing (semi-)horizontal cracks, or stop when they reach these cracks (c, experiment H5L6).

Experiment	Type of packing (Hexagonal (H) or Cubic (C))	Aggregate starting porosity (%)	Compaction rate (mm/h)	Max. stress (MPa)	Maximum strain (%)	Permanent strain (%)
H5L1	H no semi-circular discs	27.7	2.5	13.85	13.47	12.91
H5L2	H semi-circular discs	21.4	3.6	12.25	12.96	12.46
H5L3	H no semi-circular discs	27.7	3.6	18.45	12.96	12.29
H5L4	H no semi-circular discs	27.7	3.6	19.6	12.96	12.41
H5L5	H semi-circular discs	21.4	3.6	11.7	12.96	12.10
H5L6	H semi-circular discs	21.4	3.6	17.0	14.40	13.51
C5L1	C 0.2 mm radially flattened	16.4	3.6	20.3	5.21	4.47
C5L2	C 0.2 mm radially flattened	16.4	3.6	20.5	5.21	4.55
C5L3	C 0.2 mm radially flattened	16.4	3.6	26.7	5.21	4.53
C5L4	C 0.2 mm radially flattened, 45^o rotated	16.4	3.6	8.25	6.72	6.06
C5L5	C 0.2 mm radially flattened, 45^o rotated	16.4	3.6	5.33	6.72	6.20
C5L6	C 0.2 mm radially flattened, 45^o rotated	16.4	3.6	7.13	9.41	8.56
C5L7	C	21.5	3.6	8.67	7.00	6.58

Table 1. This table shows the data of all of the experiments performed on the sugar glass discs.

the ones that have the least effect of the sugar glass to steel contacts.

The cracks that form in these seven discs do not initiate at the contact point, as would be expected according to the Herzian contact theory on the stress distribution, but just outside this contact point (see Figure 12). This can be seen for both type 1 and type 2 straight cracks. Also notable is the fact that these cracks form on the side of the contact point which is the narrowest (closest to a side contact). In the outer discs these are also the places where parts break off of the discs.

3.1.2 Hexagonal packing with the presence of half discs

3.1.2a. Stress-strain development

In Figure 6b, the stress-strain diagram is shown for 5-layered hexagonal experiments on circular discs with semi-circular filler discs (experiments H5L2, H5L5, and H5L6). Since these semi-circular discs were hand cut by a knife, it was more difficult to make them the exact size. This means that the discs in the starting position did not fit exactly in their row, resulting in more open spaces and a lower number of contacts. As the sample was loaded, the discs first had to be pushed into their place, just so that all the discs had six contact points. In the stress-strain diagram, this can be recognized as a long period of low stress with increasing strain. When the discs were all pushed into position, the stress started rising rapidly and, similar to the packing without the fillers, dropped with the failure of a disc.

The first cracks form at relatively low stress. These cracks form in the filler discs in the fourth row, are horizontal and develop between the contact with the neighbouring disc from the same row and the contact between the semi-circular disc and the steel. Later, horizontal cracks form in the whole discs as well. After the discs are pushed in position and the stress starts increasing, the number of cracked discs start increasing as well (Figure 8b). The largest number of cracks form between 7.0 and 12.0 MPa. These cracks are all semi-vertical, no horizontal cracks form after the discs are pushed into their position. The same pattern can be seen in Figure 7b, where the horizontal cracks form until 9.5% strain, but the majority of the cracks form between 10% and 14% strain. The cracks that form in this latter event are all vertical.

3.1.2b Description of deformation in the discs
The horizontal cracks that form in the semi-circular discs in the first stage of the experiment are all meridional cracks. These meridional cracks are accompanied by multiple microcracks. Due to the movement of the discs along each other, some microcracks can form at these contacts (see Figure 13a).

The cracks that form when the discs have settled are mainly type 2 non-curved cracks, often accompanied by type 2 spalling or convergent cracks. These spalling and/or convergent cracks form at the same time as the non-curved cracks. At the end of all three experiments, the discs that accommodated the most amount of stress are the discs on the top row. The type 2 non-curved cracks that have formed in these discs show a Λ-shape, caused by the single sugar glass-steel contact on the top of the discs and the two sugar glass-sugar glass contact at the base of the discs. These cracks are often accompanied by type 2 spalling and convergent cracks, but some type 1 spalling cracks have formed as well. The latter cracks developed further and caused parts of the disc to break off and move into the pore space.

The discs in the middle three rows are often less deformed. Cracks in these discs can cross the already present horizontal cracks (Figure 13b), or stop at the horizontal crack (Figure 13c). The first can be seen in all three experiments, in the semi-circular discs in where horizontal cracks have formed, the latter can best be seen in experiment H5L6, where more (semi-) horizontal cracks have formed. With an increase in deformation, the amount of cracks also increases. These cracks can either be micro-, spalling, convergent, non-curved or meridional cracks and can form between contacts that already failed or between non-failed contacts.

3.1.2c Initiation of cracks
The vertical cracks that form in this experiment (type 2 straight cracks and type 2 convergent cracks) do not initiate at the positions of the original contact point, but slightly away from it (see Figure 14a). Due to the compaction, the contacts have flattened causing a broader contact area. The cracks initiate at the edges of these contact areas, on the side of the closest horizontal contact.

Horizontal cracks appear to initiate at the contact points (see Figure 14b). However, since these cracks formed at the beginning of the experiments, the contacts haven't flattened yet, resulting in slightly different contact conditions. This difference might be responsible for the difference in the position the cracks initiate.

3.1.3 Cubic packing
3.1.3a Stress-strain development
In Figure 15, the stress-strain diagram can be seen for a cubic packed aggregate of circular sugar glass discs. In the first part of the graph, the settling of the discs can be recognized by the slow increase of stress with increasing strain. After a compaction of 4.25%, the stress starts to increase.

The first crack forms around 4.9% compaction, with a stress of 2.4 MPa (see Figure 16). This continues, until at 6.6% strain, 8.5 MPa the failure of multiple discs causes a stress drop of 1.5 MPa. After this stress drop, the stress builds again and discs fail at lower stresses than previously reached.

3.1.2b Description of deformation in the discs
Most of the cracks that form in this cubic experiment are meridional cracks, often accompanied by convergent cracks. In a later stage (after 6.0% strain), spalling cracks start to form. The first three discs fail at the same time. These discs are in the bottom right side of the packing (discs {1,5}, {2,5}, {3,5}) and contain meridional cracks. However, all three contain microcracks at either one of or on both the top and bottom contact. Later, more meridional and convergent cracks form between the same contact areas as the first ones have formed.

Near the end of the experiment, the difference between the outer discs, the ones on contact with the steel, and the inner nine discs is very small. Two discs remained visibly undeformed: discs {1,1} and {1,4}, both on the bottom row.

3.1.3c Initiation of cracks
The meridional cracks and the convergent cracks all form between the top and bottom contact. If a disc contains one meridional crack,

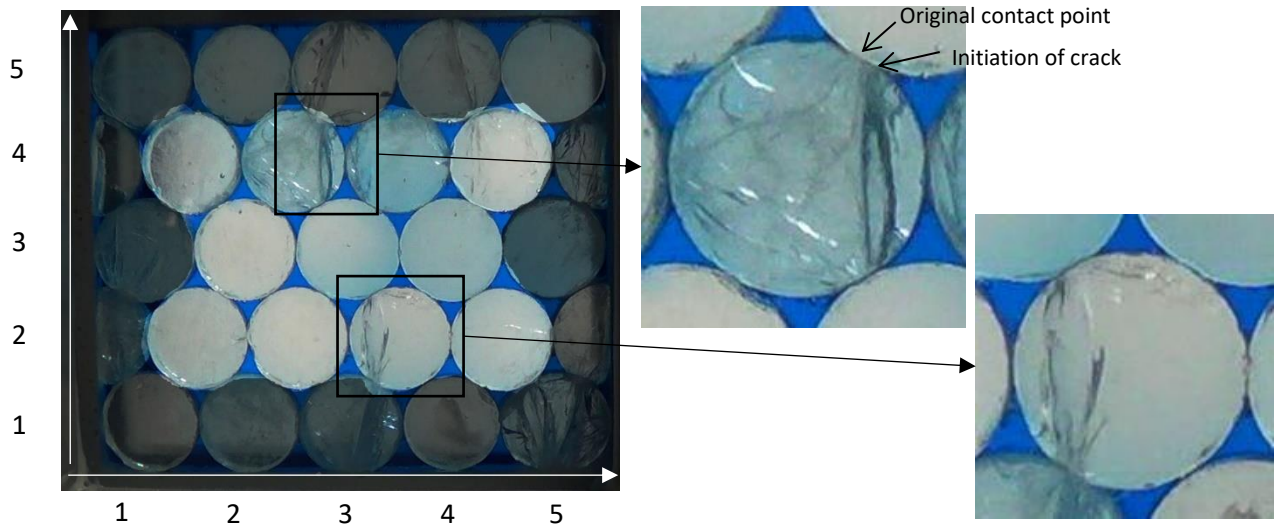

Figure 14. Two examples of places where cracks formed in experiment H5L5. In both discs the cracks didn't form exactly at the contact point, but slightly away from it, both on the narrowest side of the disc.

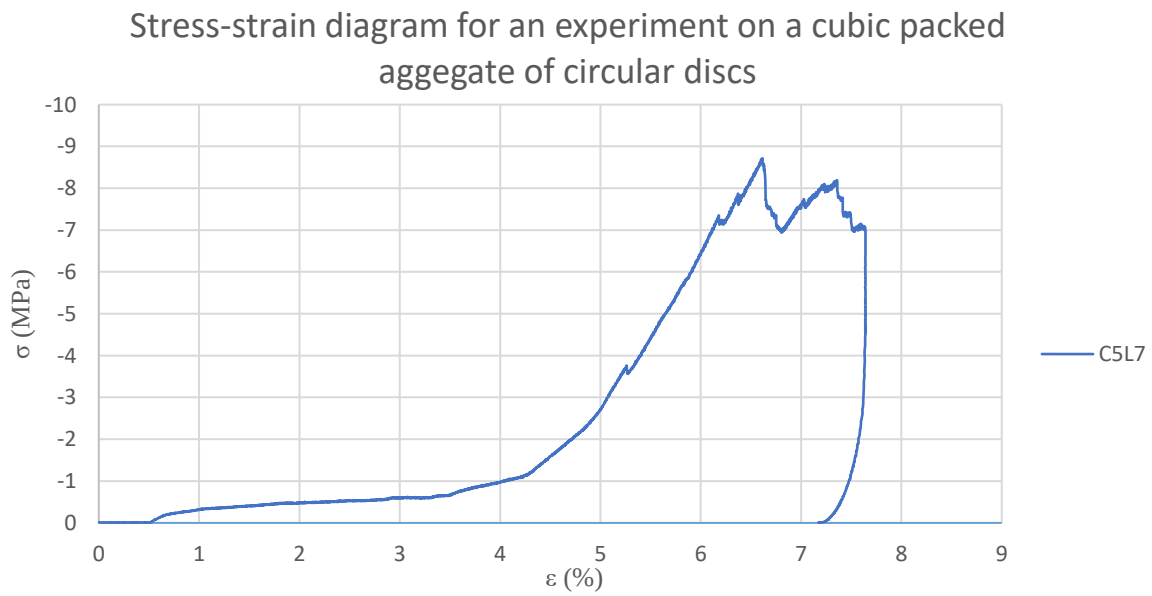

Figure 15. The stress-strain diagram of an experiment performed on cubic packed circular discs. Note that in this diagram, negative stress displays compaction.

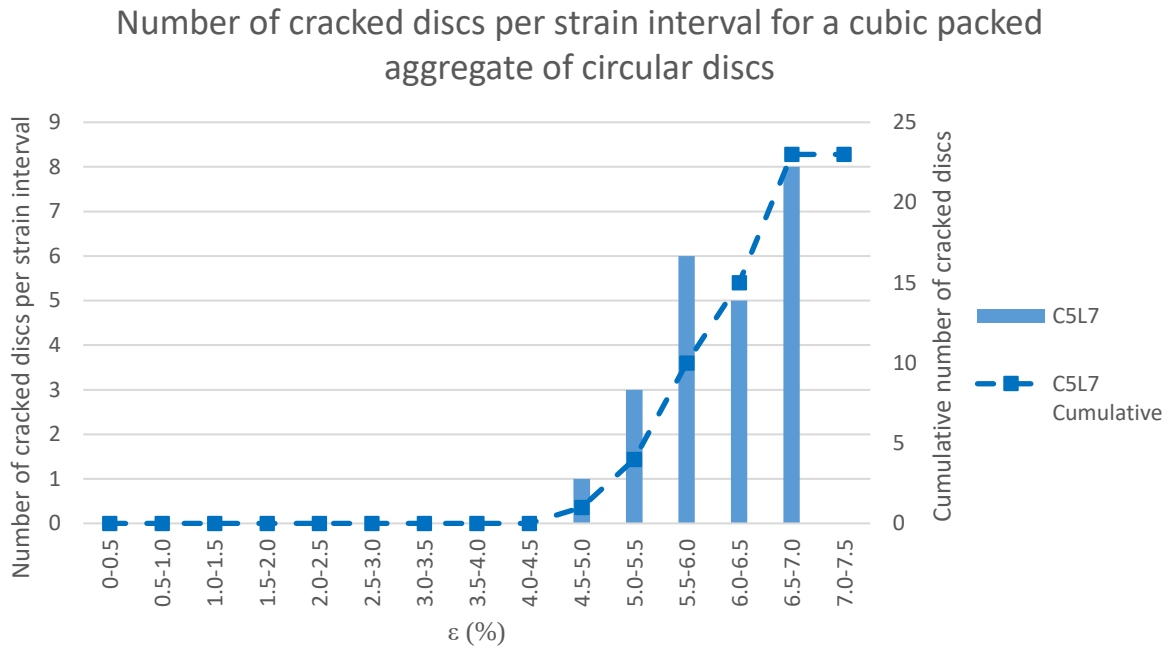

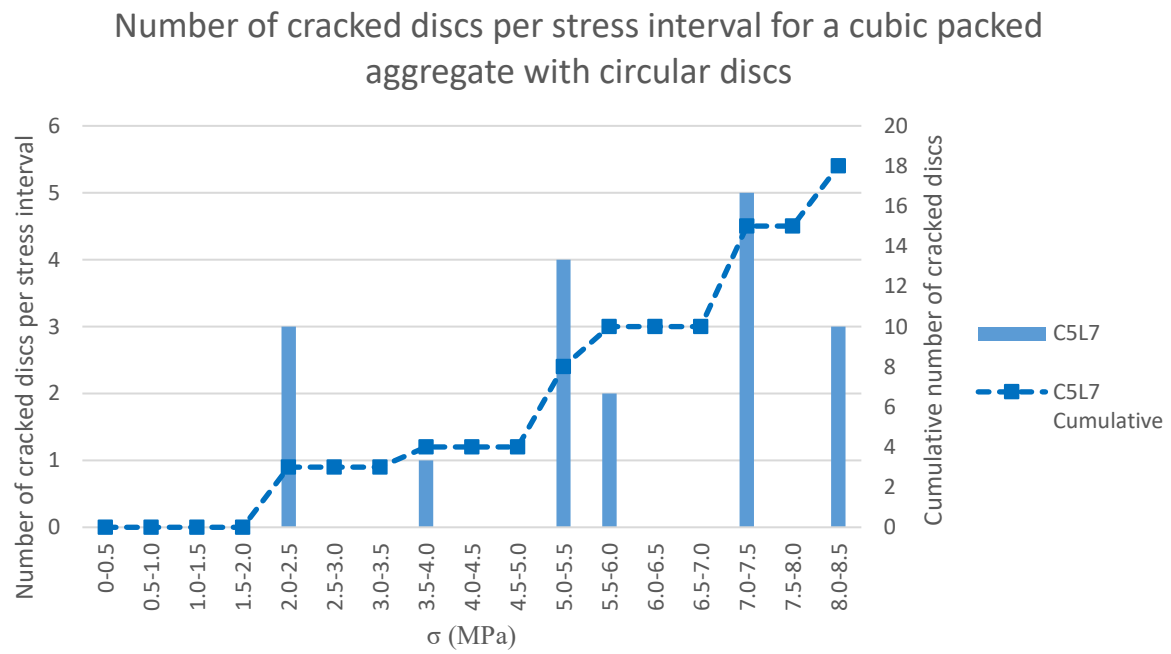

Figure 16. The development of number of failed discs per strain (a) or stress (b) interval, as well as the development of cumulative number of failed discs with changing strain or stress.

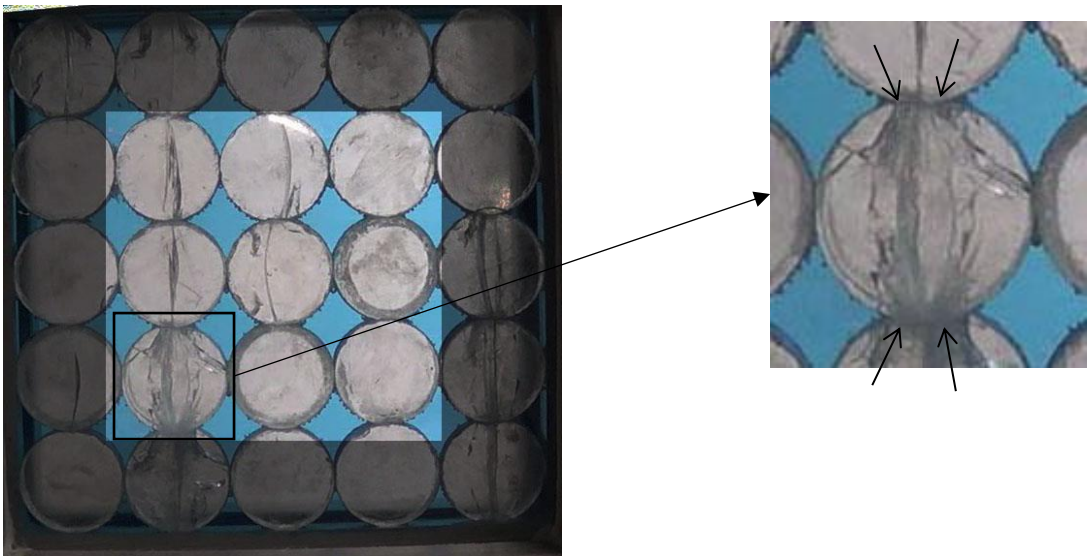

Figure 17. Multiple cracks formed in one disc: meridional cracks accompanied by convergent cracks and spalling cracks. Notable is that these cracks initiate at two different positions along the top and bottom contacts, indicated by arrows.

this fracture initiates at the contact point between two discs. However, when multiple meridional crack form in one disc, accompanied by convergent cracks, these initiate at different parts along a broader contact zone (see Figure 17). The spalling cracks that formed in the disc shown in this Figure formed from two different part along the top contact as well: they formed at the same places along the top contact where the meridional and convergent cracks formed, on the side closest to the contact with the side disc that the spalling cracks formed between.

3.2. Sugar glass experiments on flattened discs: cubic packing

3.2.1 Regular cubic packing, 2.8 mm contact length, porosity of 16.4%

3.2.1a Stress-strain development

In Figure 18 the stress-strain curve can be seen of the experiments performed on cubic packed discs, where the contact areas between the discs have been flattened by 0.2 mm, forming a contact length of 2.8 mm (experiments C5L1, C5L2 and C5L3). When studying the patterns formed by the stress-strain curve, it becomes clear that the compressional stress increases quickly with increasing strain. This increase takes place after initial resettling of the discs into the more stable positions from which they are unable to move any further. This resettling stage is a lot shorter than the resettling stage that is observed in the previously described hexagonal and cubic experiments.

Cracking of the discs takes place at lower stress and strain levels than the hexagonal experiments: the first crack forms at a strain of 0.4% (Figure 19a) and a stress of 1.0 MPa (Figure 20a). The majority of the discs fail between a strain of 1.0% and 3.5%. This is caused by the fact that this Figure shows the undeformed discs that fail, while cracks in already failed discs are not displayed. After a strain of 4.0%, an average of 22 discs out of 25 have failed. This means that further deformation in these discs is not taken into account in this Figure. The deformation of these discs after this point can however be seen in the Appendix, where the pattern of the cracked discs is further highlighted. The development of cracks can also be studied in Figures 21a and 22a, where the number of cracks in the central nine discs (the discs without a steel contact) are counted. This gives a better overview about the development of cracks in the different experiments. Here it can be seen that the cracks forming at the start of the experiment are mainly in the discs in contact with the steel. Another feature that can be observed is that the number of cracks keep increasing towards the end of the experiment, which was not visible in Figure 19 (e.g. the pattern of experiment H5L6).

The pattern of cracked discs per stress interval looks very similar (Figure 20). Again,

a)

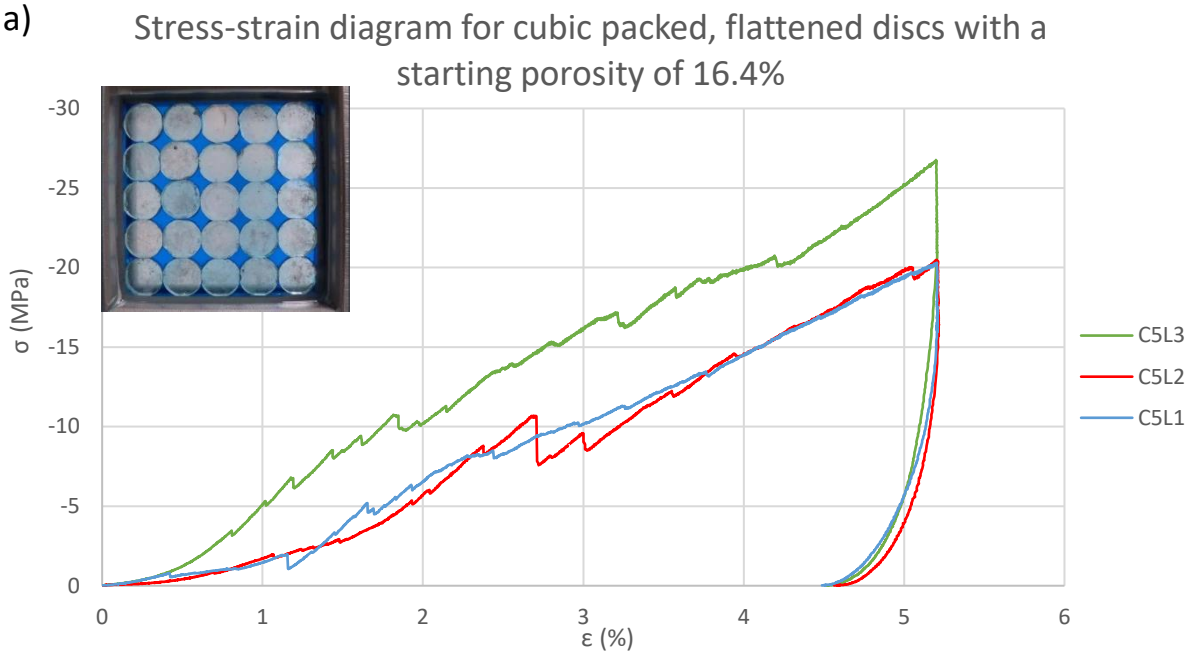

b)

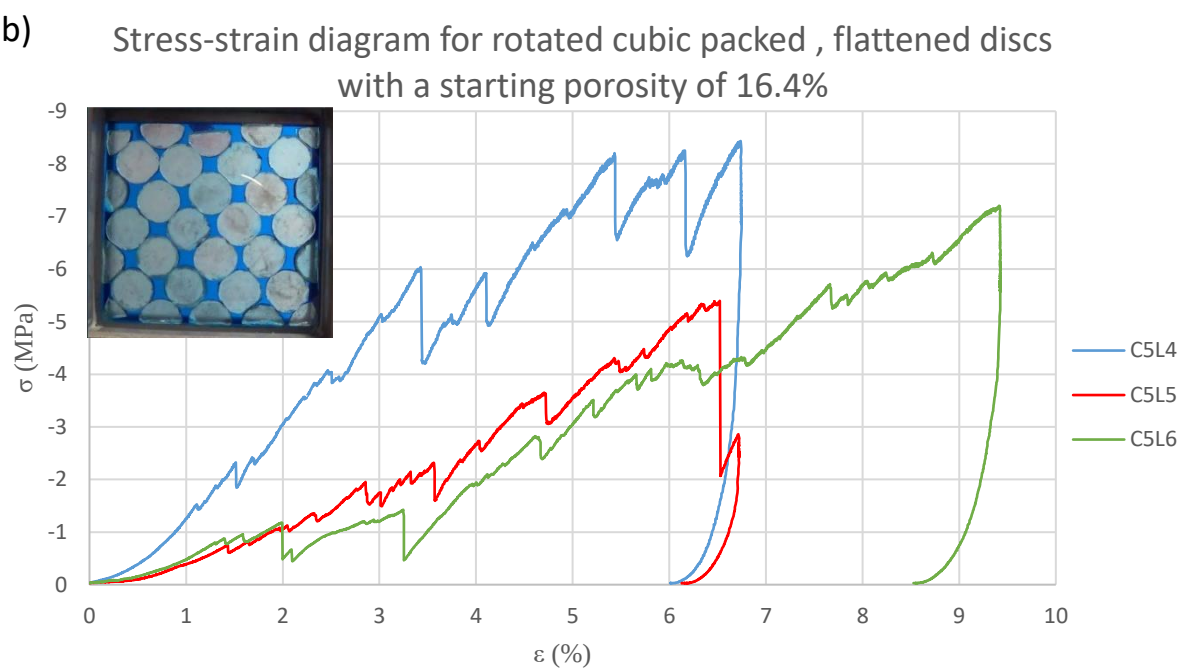

Figure 18. The σ-ε diagrams for the cubic experiments: (a) for a normal cubic packing with flattened contacts, (b) for a 45° rotated cubic packing with flattened contacts and (c) for normal cubic packing on circular discs. Note that compressional stress has been taken negative, hence the negative values on the y-axis.

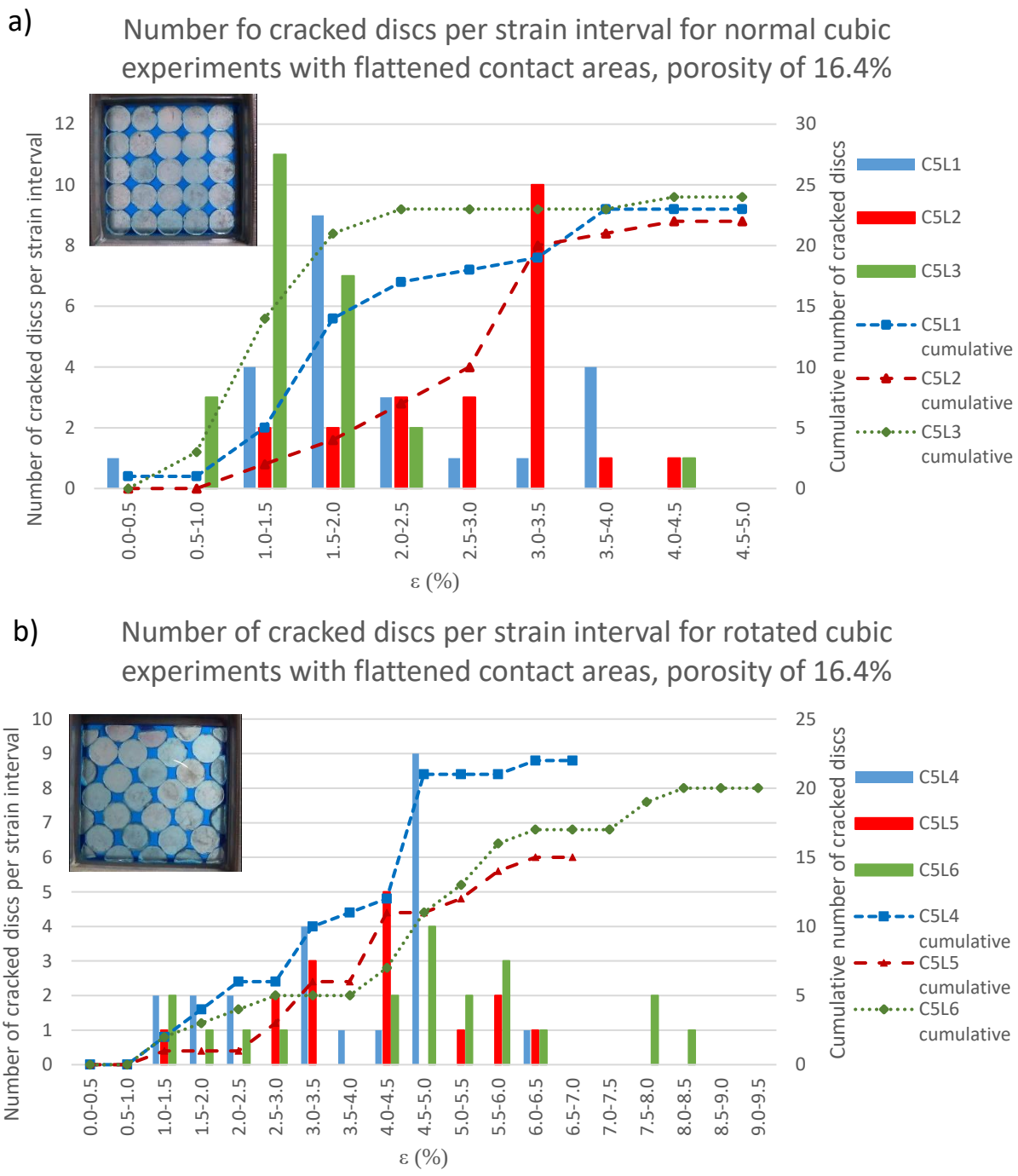

Figure 19. The number of discs that failed per strain interval during the cubic experiments, shown per experiment: in (a) the number of failed discs are shown for the normal cubic packing with flattened contacts, in (b) the number of cracked discs for a rotated cubic packing with flattened contacts.

a)

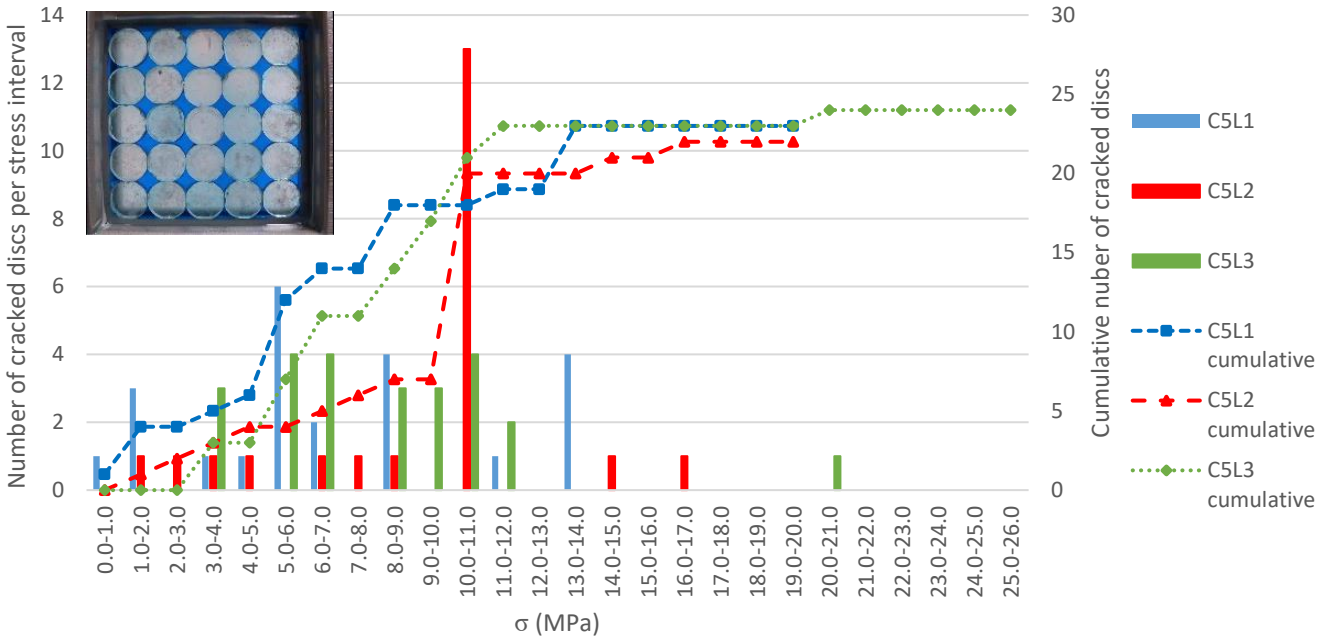

b)

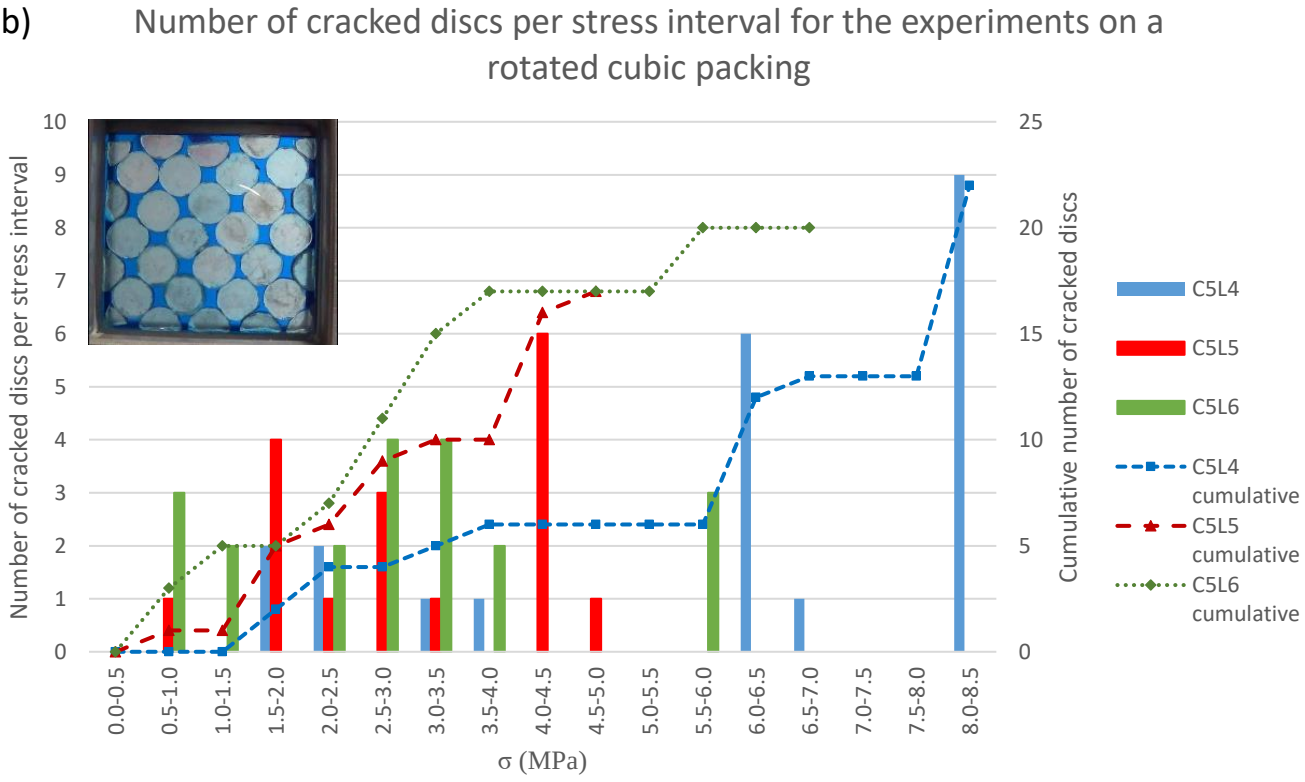

Figure 20. The number of discs that failed per stress interval during the cubic experiments, shown per experiment.

a)

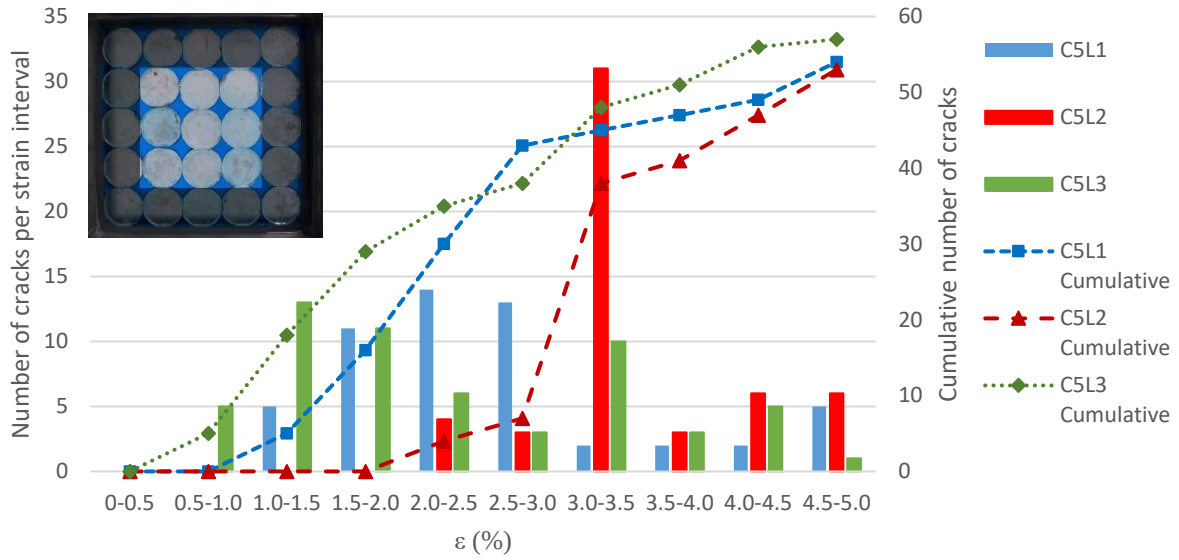

b)

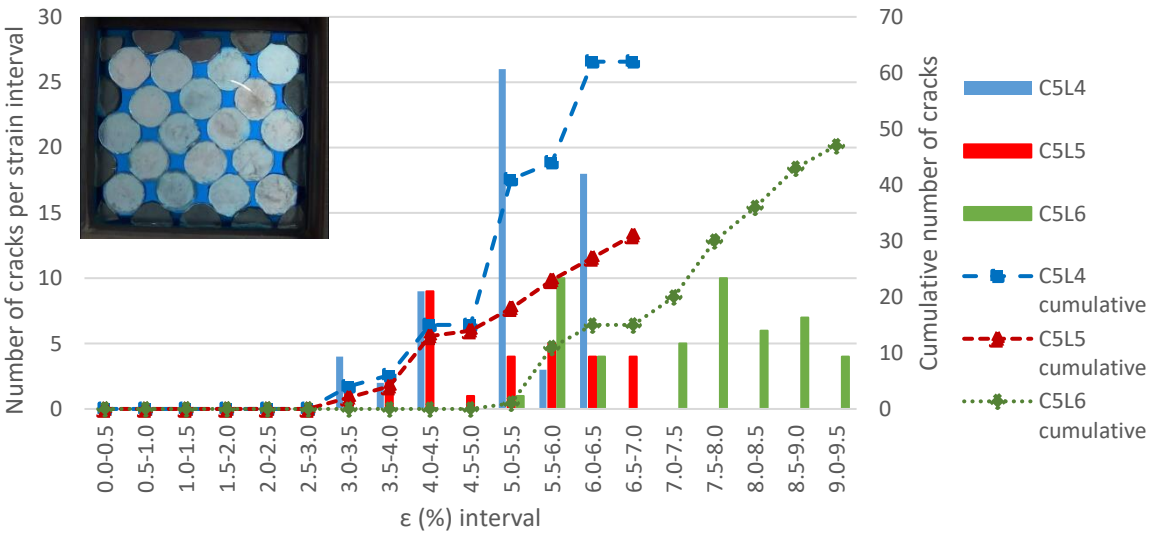

Figure 21. The number of cracks per strain interval for a cubic packing with flattened sides (a) or for a rotated cubic packing with flattened sides. Only the cracks in the central 9 and 18 discs respectively are counted, since these are the discs with the least amount of influence of the steel boundary.

a)

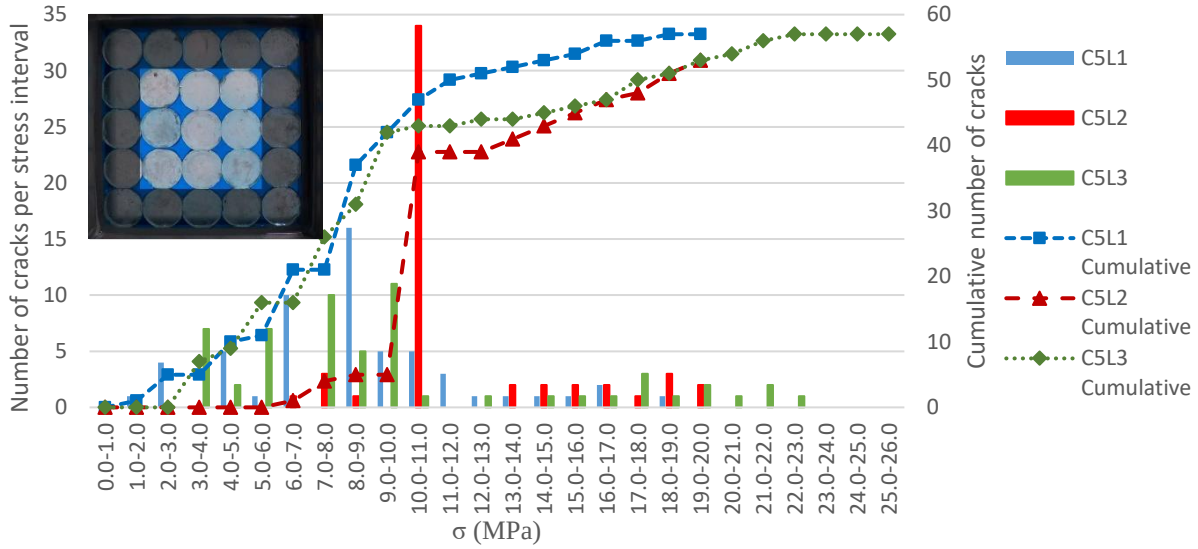

b)

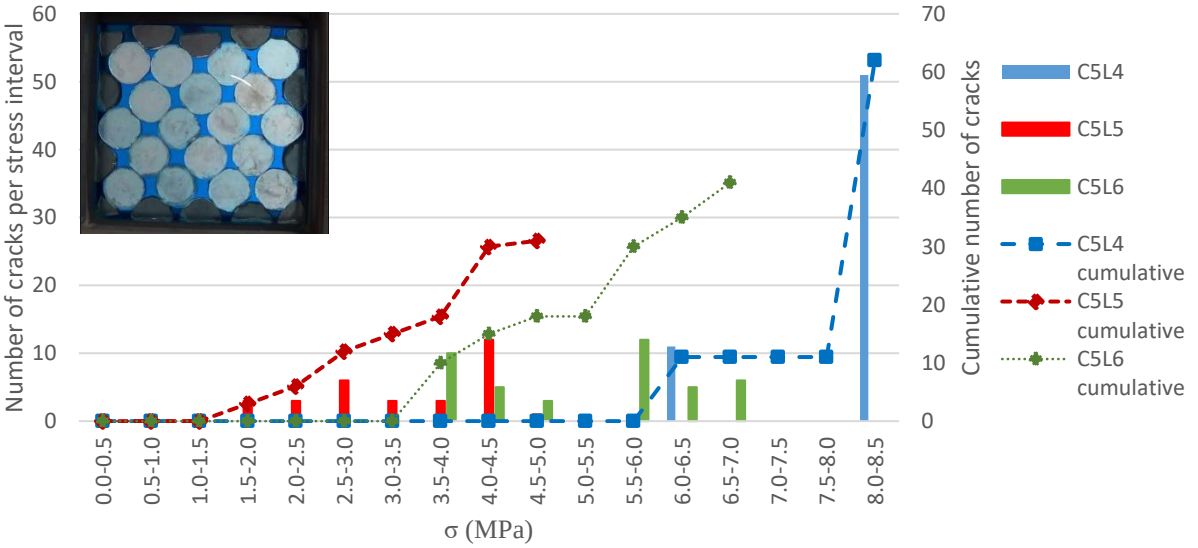

Figure 22. The number of cracks per stress interval for a cubic packing with flattened sides (a) or for a rotated cubic packing with flattened sides. Only the cracks in the central 9 and 18 discs respectively are counted, since these are the discs with the least amount of influence of the steel boundary.

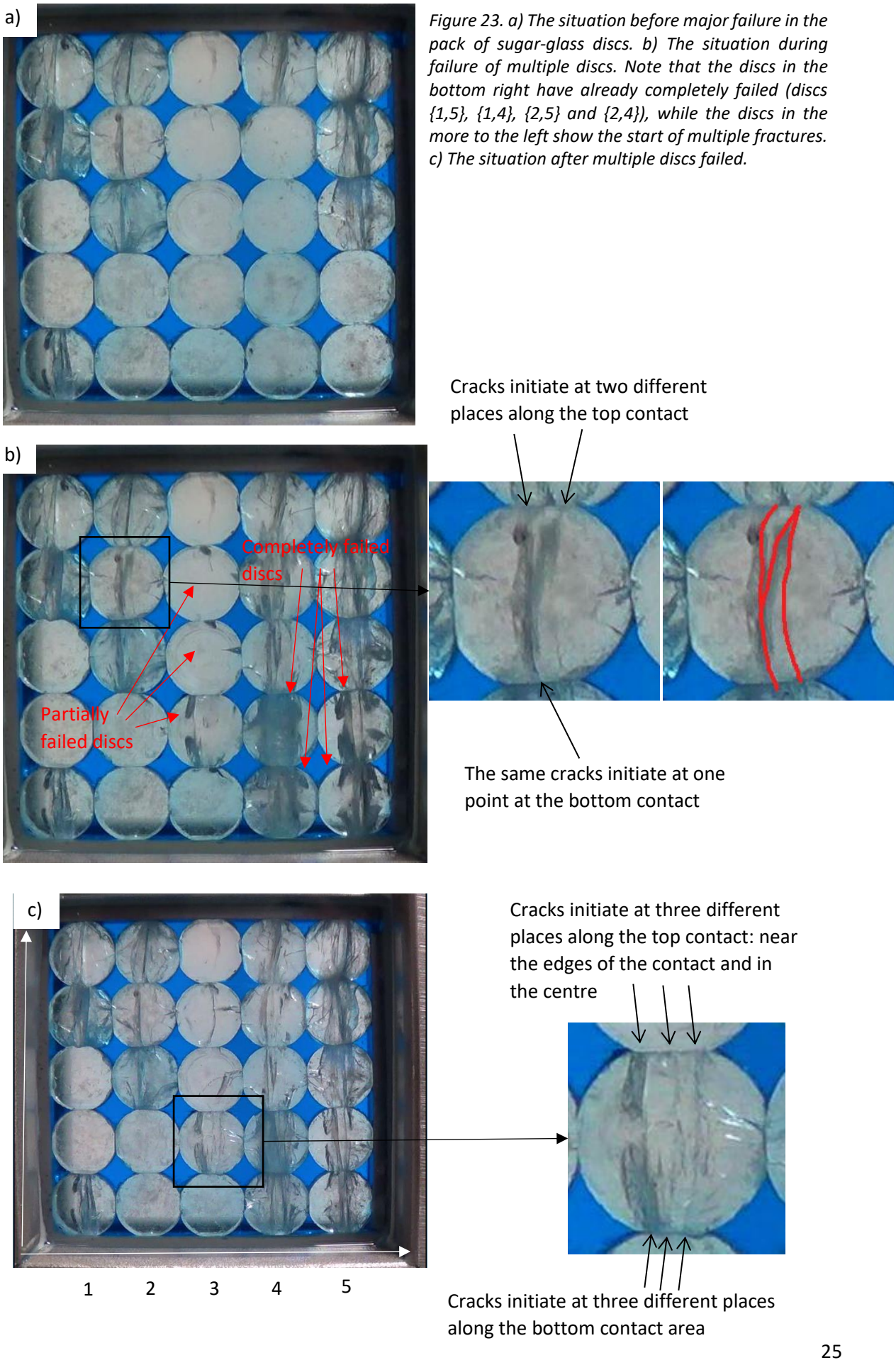

Figure 23. a) The situation before major failure in the pack of sugar-glass discs. b) The situation during failure of multiple discs. Note that the discs in the bottom right have already completely failed (discs {1,5}, {1,4}, {2,5} and {2,4}), while the discs in the more to the left show the start of multiple fractures. c) The situation after multiple discs failed.

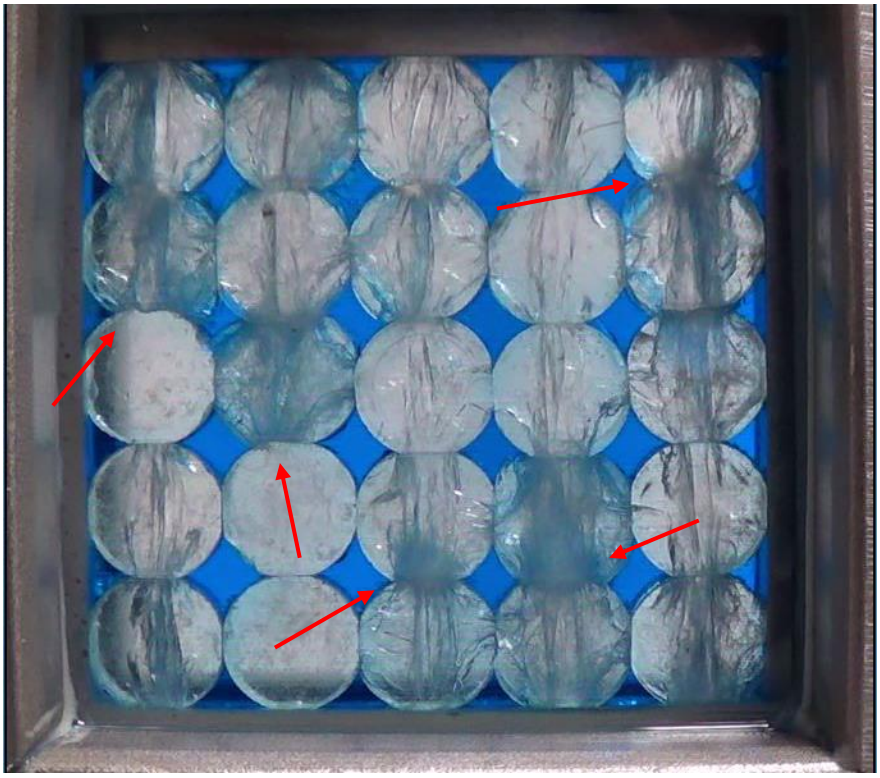

Figure 24. The final situation after deforming sample C5L2. Note the contacts where deformation was concentrated during the loading, indicated by the red arrows.

most discs fail in an early stage, again caused by the method of displaying only the undeformed discs that fail. After MPa, an average of 22 out of 25 discs have failed, which means that most of the deformation that takes place in the discs is concentrated in the already failed discs. Most discs fail between 6.0 and 7.0 MPa. In Figure 22, the number of cracks per strain interval are shown. These show that the number of cracks in the central 9 discs increase towards the end as well. This Figure shows differences to Figure 20 which are similar to the differences between Figure 19 and Figure 21.

3.2.1b Description of deformation in the discs

The majority of the cracks that form in these three experiments are vertical cracks, either meridional or convergent cracks. These cracks all formed between two contact surfaces. Spalling cracks can be recognized as well, but they form in a later stage during deformation. The height of the row has a big influence on the disc that fails first: due to the fact that the discs were hand-filed, there might be slight differences between the height of the column of discs. Within the highest column the first failed disc can be found.

After a build-up of stress in the packing and the failure of single discs, at 2.7% strain and 10.6MPa stress a big failure event occurs where many (>6) discs fail within 0.033s (one frame). Due to the development of the cracks within these discs it is possible to identify which disc failed first. This can be seen in Figure 23, where three images show the situation in C5L2 just before, during, and just after failure. What can be seen is that the discs in the bottom right of the packing have already failed while the discs more to the top left of these discs only show minor cracks on the places where later the cracks will form. This shows that for this case deformation moved from the bottom right to the top left.

After multiple discs failed in a column, the deformation starts to concentrate in a specific disc or at a specific contact. This can be seen in Figure 24, where the end of the experiment is shown for C5L2. In this Figure, the arrows point to zones where deformation was concentrated. These zones can be recognized by the multitude of microcracks in the discs/near the contacts. Two out of the three discs that remained undeformed during the experiment share a contact with this highly deformed area.

3.2.1c Initiation of cracks

The images in Figure 23 can be used to find more information about the position cracks initiate. What can be seen is that the cracks all

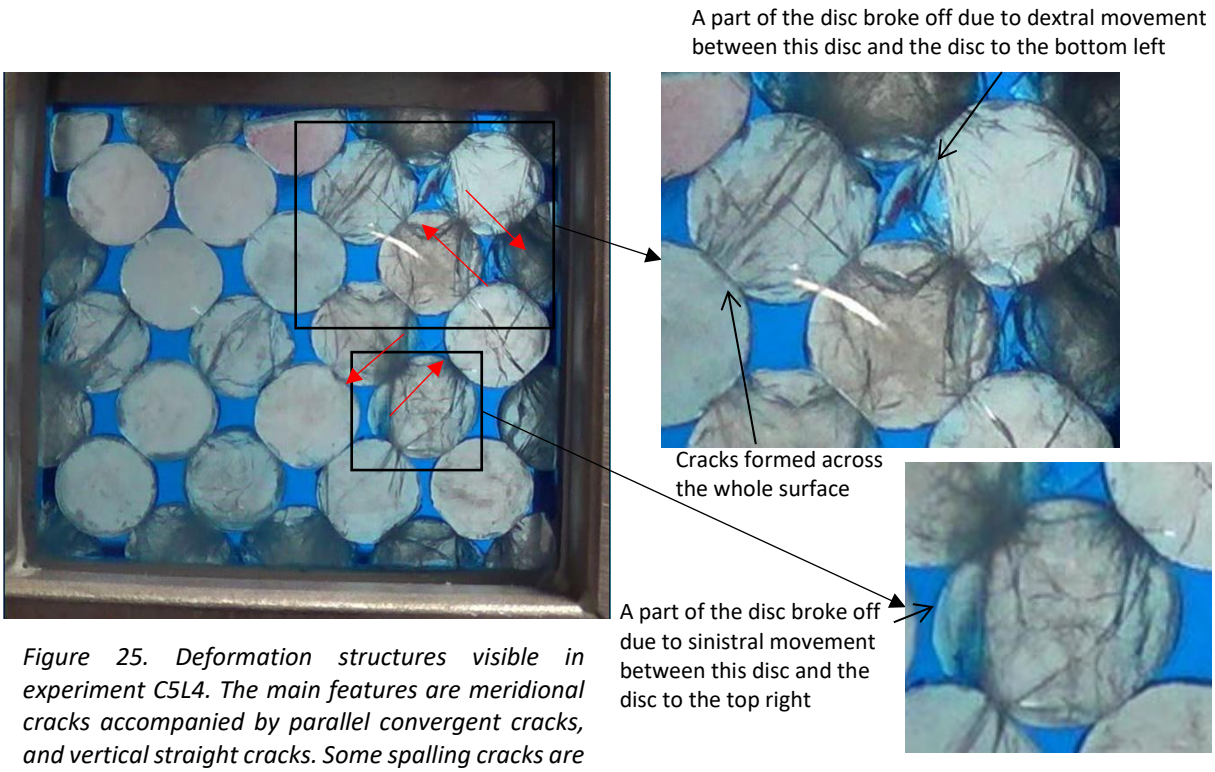

Figure 25. Deformation structures visible in experiment C5L4. The main features are meridional cracks accompanied by parallel convergent cracks, and vertical straight cracks. Some spalling cracks are visible in the discs. With red arrows, the relative movement of the discs is shown, which is caused by the vertical oriented stress on the system. This movement caused the failure of discs on the narrow side and a vertical straight crack formed between (in these cases) the top and bottom left contacts.

form at the contact area between two discs, but the position along this contact varies. The cracks can form at the edges of the contact area or in the middle, multiple cracks can form between the same two positions or can form at the same position at one contact, but at different positions at the other contact.

3.2.2 Rotated cubic packing, 2.8 mm contact length, porosity of 16.4%

3.2.2a Stress-strain development

For this set of experiments, an aggregate was made that consists of a 45° rotated cubic packing. The discs that were in contact with the steel all consisted of semi-circular or quarter filler discs (see Figure 1c), which were hand-cut. This again caused a slow increase of stress at the start of the experiment (see Figure 18b). However, the settling of the discs didn't take as long as observed in the hexagonal experiments.

The first discs failed at relatively low stress and strain: at 1.5MPa and 1.1%, at 0.75MPa and 1.4%, and at 0.85MPa and 1.4% for experiments C5L4, C5L5 and C5L6 respectively. With increasing stress, more discs fail. However, the first discs that fail are mainly the outer semi-circular or quarter discs. This becomes visible when comparing Figures 19b and 20b with Figures 21b and 22b respectively. Figures 19 and 20 show the number of failed discs changing with increasing strain or stress, while Figures 21 and 22 focus on the number of cracks in the discs without a sugar glass-steel contact. Up to 3% strain and 1.5MPa, no cracks have formed in these central discs in any of the experiments.

3.2.2b Description of deformation in the discs

As mentioned previously, the first discs to fail are the semi-circular and quarter discs along the edges of the aggregate. The cracks that form in these discs are mainly meridional cracks forming between the contact with the sugar glass and the steel. The cracks that form in the inner 18 discs are mainly meridional and convergent cracks. However, spalling cracks form within these discs as well (see Figure 25).

Since the experiment is a uniaxial one, the left and right steel boundary are fixed. This largely prevents the sliding of the discs along each other. However, due to the major deformation in the semi-circular discs on the side, sliding occurs along certain contacts. In

Figure 25, these contacts are indicated with red arrows, showing the slip direction of both discs. The slip along the contact surface influences the formation of cracks: cracks form between the narrow (the part with the smallest area of sugar glass) side of the disc and the contact below it. This narrow part of sugar glass often breaks off of the original disc to move into the pore space.

3.2.2c Initiation of cracks

Similar to all of the previous experiments, the cracks form between two different contact areas. Meridional and convergent cracks can form all across the contact surface (see Figure 25) The vertical straight cracks all form on the narrow part of the sugar glass disc. This same behaviour can also be observed in most spalling cracks.

4. Microstructural analysis of deformed sand aggregates

4.1 Heksenberg sand of 275 +/- 25 mu (Brzesowsky et al, 2014)

The quartz sand grains visible in Figures 26, 27 and 28 have been uniaxially deformed by Brzesowsky et al. (2014a). The sand was obtained from the Heksenberg Formation, Beaujean quarry, Netherlands and consists of > 99 wt% quartz (Brzesowsky et al, 2011), most grains were subrounded at the start of the experiments and sieved to obtain a grain size of 275 ± 25 µm. Both samples were first deformed dry for two days, and after another 10 (BS31) or 11 (BS32) days, with water as a pore fluid. BS31 was compressed with 30MPa, while BS32 was compressed with 21.7 MPa. This stress difference resulted into a lower crack density in BS32 (90% in BS31 vs. 50% in BS32, Brzesowsky et al. (2014)).

Most cracks that have formed in sample BS32 make an oblique angle with the compaction direction. Since the micrographs are viewed in 2D and the cracks are 3D features, it is not reliable to measure said angles. Cracks run from one grain contact to another, some cracks continue through multiple grains (see Figure 27a). Other grains show palm tree-like structures, where cracks originate in one point and scatter to different contacts or places along one contact (Figure 27b). These sets of cracks can run parallel to each other. When the cracks grow larger, the grain can disintegrate into separate pieces, which all deform and rotate differently (see Figure 27c), creating a smaller grain size.

Due to a higher stress during deformation, more cracks have formed in sample BS31 (see Figure 26). Most of the cracks developed in this sample have formed with a similar angle with the compaction direction as the sand deformed at lower stress (BS32). In Figure 28a, a microscope image is shown of a quartz grain containing a horizontal meridional crack and two horizontal convergent cracks. On the left side, the grain underwent intense deformation and formed a crushed contact region. The deformed grain that can be seen in Figure 28b shows a type 1 meridional crack. The top part of this circular grain consists of

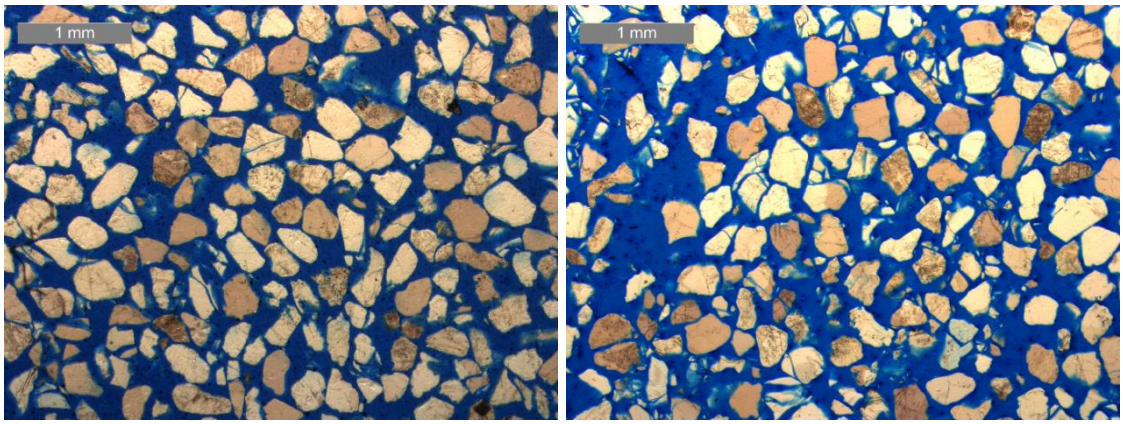

Figure 26. Microscope images of deformed loose quartz sand with an initial grain size of 275 ± 25 µm. On the left sample BS32 is visible, which has been deformed at 21.7 MPa, on the right sample BS31 is shown, which has been deformed at 30 MPa (Brzesowsky et al., 2014a, Table 1). Both samples contain water as a pore fluid. The compaction direction is vertical.

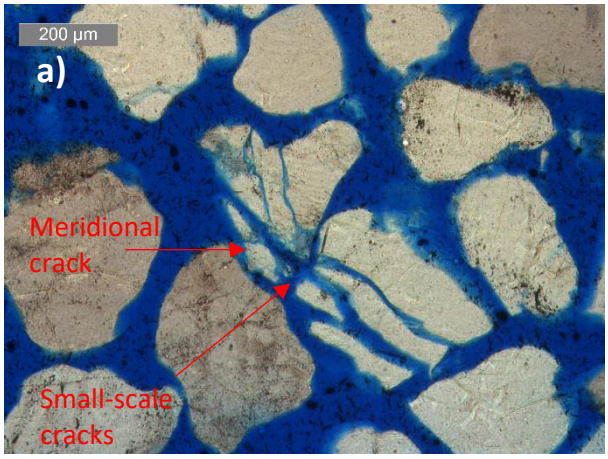

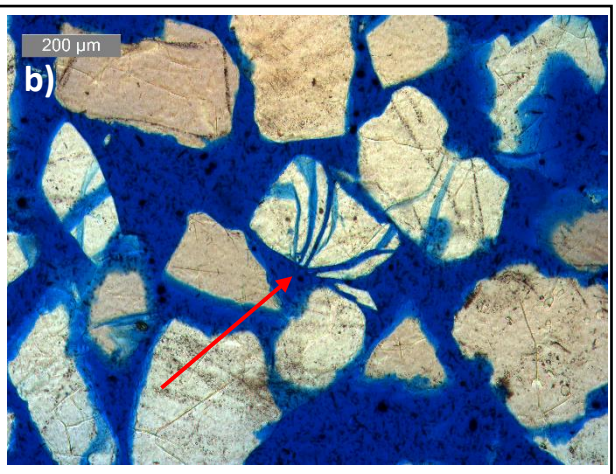

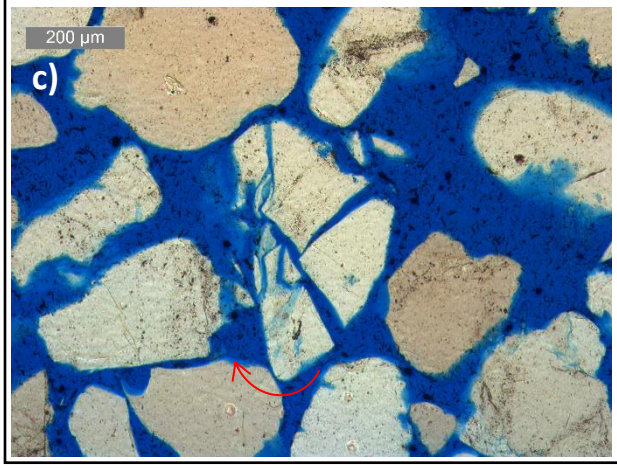

Figure 27. Micrographs of sample BS32, which has been deformed with 21.7 MPa. Compaction direction is vertical. a) Two grains in which meridional cracks developed. One crack continues through both grains. The contact region between the two failed grains consists of multiple small-scale cracks. b) Multiple sets of divergent cracks that have formed in a grain (indicated by the red arrow), forming a palm tree-like structure. These cracks originate in one point, and end at different contacts. c) A sand grain that has been broken into separate pieces, which then all have rotated separately. This rotation could have occurred during deformation, but can also be an effect of the preparation of the sample.

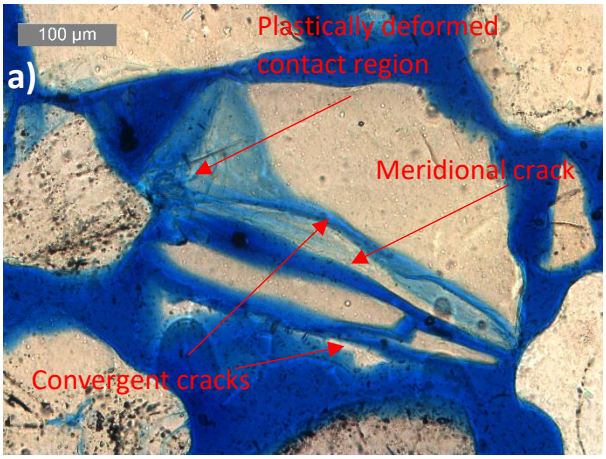

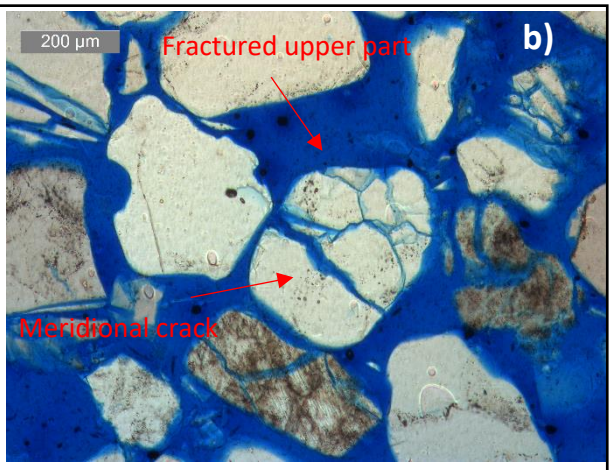

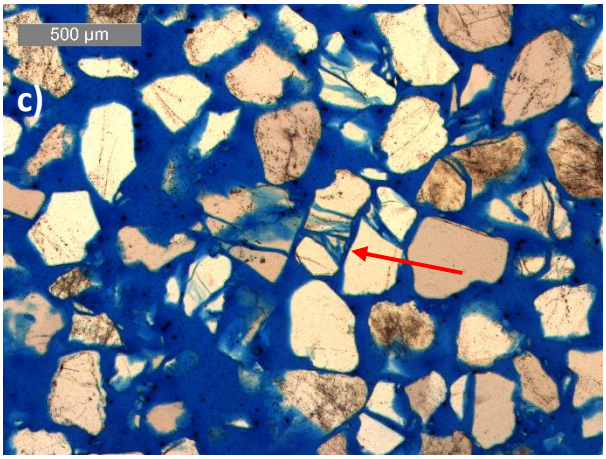

Figure 28. Micrographs of sample BS31, which has been deformed at 30 MPa. The compaction direction is vertical. a) A failed sand grain showing multiple sets of cracks (meridional and convergent cracks) which all originate and end at the same contact. At the left contact, a plastically deformed region can be identified. b) A sub-rounded grain in which a meridional crack has formed. The upper part of the grain contains a lot of microcracks while the lower part remains visually undeformed. c) In the grain in the middle (with the red arrow), multiple meridional and divergent cracks have formed between two broad contact surfaces.

Figure 29. a) A microscope image of deformed loose quartz sand with an initial grain size of 425 ± 25 µm, deformed with water as a pore fluid. The following images are close ups of different parts of the same sand aggregate. After Hangx et al. (2010). b) The grain in the centre is heavily deformed, resulting into multiple meridional cracks and spalling cracks. All these cracks appear to have grown between contact surfaces. c) The type of contact between two grains can change along this surface. In this image, the top part of the contact is a sutured one, while after ± 200 µm the contact changes to a failed surface. Here the grain consists of many parallel meridional cracks. d) The two encircled grains contain a crack that runs through both grains. In the right grain, this crack combines with another crack. This configuration is similar to the one that can be seen in Figure 28c. The compaction direction in these images is vertical.

type 2 meridional cracks and divergent cracks, while the bottom part appears to be undeformed. In Figure 28c multiple failed grains can be seen that show relatively shallow-angle cracks. The grain in the middle contains multiple meridional cracks together with some divergent cracks. These cracks have formed between the same broad contacts with the neighbouring grains. Other grains in the image show meridional cracks that halfway in the grain split into two cracks, that end at the same surface.

4.2 Heksenberg sand of 425 +/- 25 mu (Hangx et al, 2010)

In Figure 29 loose quartz sand grains (grain size of 425 ± 25 µm) are shown which were deformed with water as a pore fluid with an effective stress of 35.5 MPa. The pore fluid pressure was kept at atmospheric pressure throughout the experiment. The quartz sand originates from Heksenberg Formation as well, and the grains are well-rounded as well. According to Hangx et al. (2010, Figure 13) the percentage of cracked grains in the wet samples is 75%. This is a lower percentage than the one that can be found in experiment BS31 of Brzesowsky (90%), but it is higher than the percentage that can be found in experiment BS32 (50%, Brzesowsky et al., 2014a), even though the stress used in Hangx's experiment

was higher (35.5 vs 30.0 and 21.7 MPa respectively). The amount of horizontal cracks in these sections is higher, while the amount of vertical cracks is lower than in the samples discussed above. However, it should be noted again that the angles of the cracks could be different due to the possible changes when viewing 3D structures in a 2D image.

In Figure 29b-d, close-ups of the structures in deformed sand grains are shown. Most of these failed grains contain meridional and divergent cracks that run from one contact surface to another (Figure 29b) or continue through multiple grains (e.g. Figure 29d). The contact surfaces between the grains in the sample can either be sutured or failed. In Figure 29c it can be seen that the type of contact between two grains can change: in the left the contact is sutured, while ± 200 µm to the right the grain is broken at the contact.

5. Discussion

5.1 Differences between the same type of experiments

5.1.1 Hexagonal without semi-circular fillers

The first major difference that arises is when experiment H5L1 is compared to the other two experiments. The difference in compaction rate (2.5 mm/h for H5L1 and 3.6 mm/h for H5L3 and H5L4, see Table 1) caused a big difference in stress-strain behaviour, as well in the cracking behaviour. For the same strain, the stresses are much lower. Before the first large cracks form in experiment H5L1, the compaction takes place at the contacts as flattening while no cracks form between different contacts. This flattening phase can be seen in experiments H5L3 and H5L4 as well, but in the latter two experiments discs fail at an earlier stage, at lower stress and strain. This can be seen in Figure 11, where an image of H5L1 is shown at a strain of 10.5% which can be compared to an image of H5L3 at the same strain. Here, the discs of H5L1 all have flattened contacts, while experiment H5L3 consists of discs that have both failed and gotten flattened contacts. After 11.0% strain, the first discs start to fail, but the total amount of failed discs is still lower than in experiments H5L3 and H5L4 (see Figure 7).

5.1.2Hexagonal with semi-circular fillers

In experiments H5L2 and H5L5 the stress-strain development is very similar, with first a small increase in stress, followed by an increase after the discs are pushed into position. The curve of experiment H5L6 has a different pattern. The smaller increase of stress continues for a longer time, but the increase of stress is of a bigger magnitude. Furthermore, the stress drops caused by the fracture of the discs are much smaller and are much faster restored than the ones in experiments H5L2 and H5L5. This leads to a higher maximum stress. This difference can partially be explained by the starting situation: in experiment H5L6 the sugar discs didn't fit in nice rows, resulting in an even longer time necessary for the rapid build-up of the load. Since the sides of the experimental cells were fixed, the discs couldn't expand outwards to make place for the discs pushed down. This can explain the higher number of horizontal cracks that are observed in experiment H5L6, since the vertical stress is expected to be much higher due to this lack of horizontal space.

5.1.3 Normal cubic with flattened contacts

A first difference between experiments C5L1, C5L2 and C5L3 can be seen in the stress-strain diagram (Figure 18). Here it can be noted that experiments C5L1 and C5L2 behave similarly, apart from the stress drop that can be observed in C5L2 at a strain of 2.7%. This stress drop can be related to the sudden failure of discs that can be recognized in Figures 19 and 20, where an increase of cracked discs can be seen at the strain interval 2.5%-3.0% and at a stress-level of 11 MPa. This stress drop cannot be recognized in experiment C5L1.

Another difference is the overall higher stress during experiment C5L3 compared to the other two experiments. The origin of this stress difference cannot be explained by the setup, as was the case with the hexagonal experiments, since all of the discs in all three cubic experiments were already at their best fit positions at the start of the experiment. In C5L3, the number of failed discs at the end of the experiment is also higher than in the other two experiments: in C5L3 24 out of 25 discs have failed, in C5L2 22 discs had failed and in C5L1 23 discs had failed. This can best be explained by the higher stress throughout the

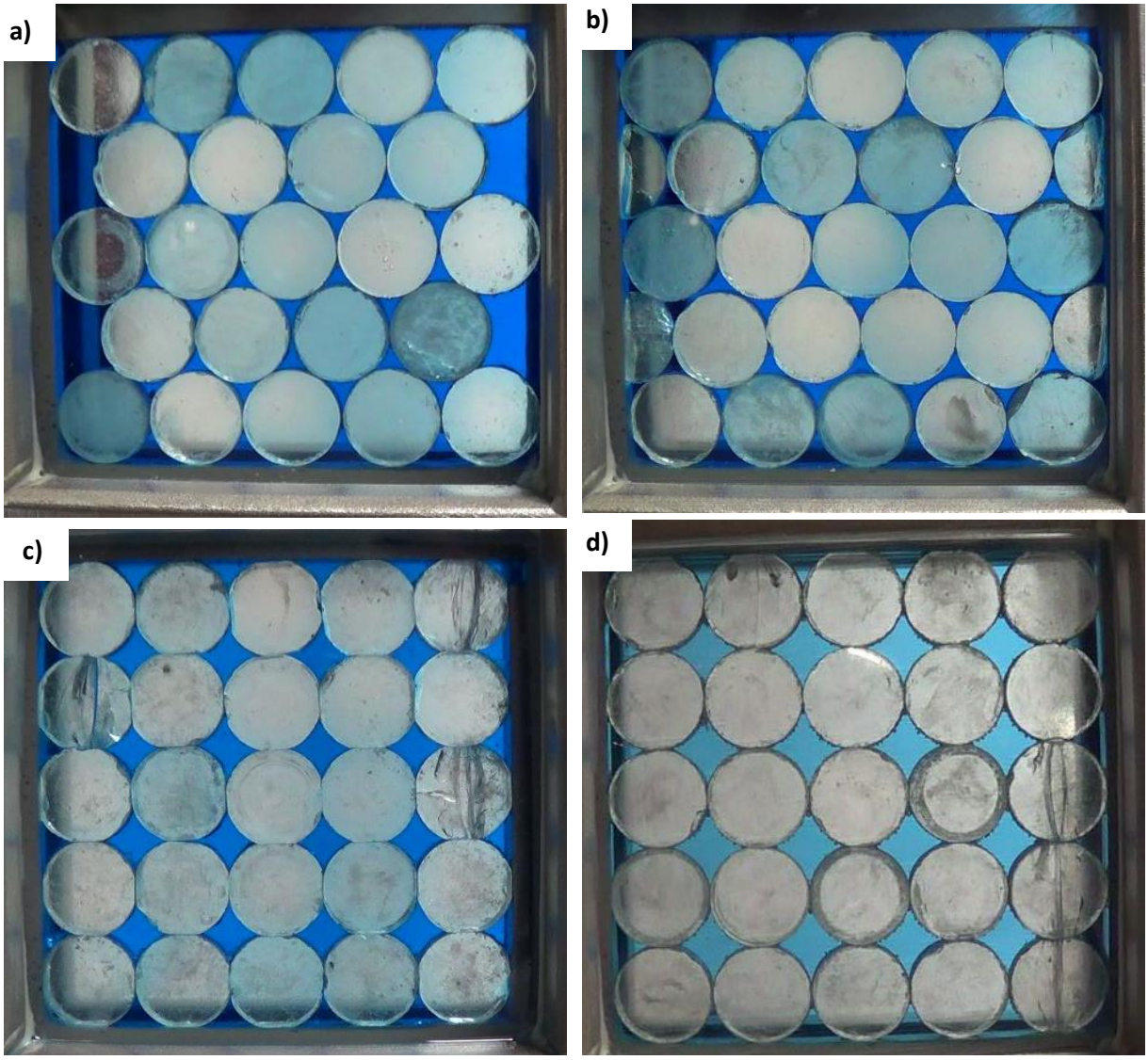

Figure 30. The five different type of experiments at a stress of 4.0 MPa. What can be seen is that in none of the experiments the discs that aren't in contact with the steel have failed. However, a difference can be seen in the outer discs: where in the hexagonal experiments (a and b) maximum one semi-circular disc has failed, in the cubic experiments (c, d and e) multiple (semi-circular) discs have failed.

(a) Experiment H5L4
(b) Experiment H5L5
(c) Experiment C5L2
(d) Experiment C5L7
(e) Experiment C5L4

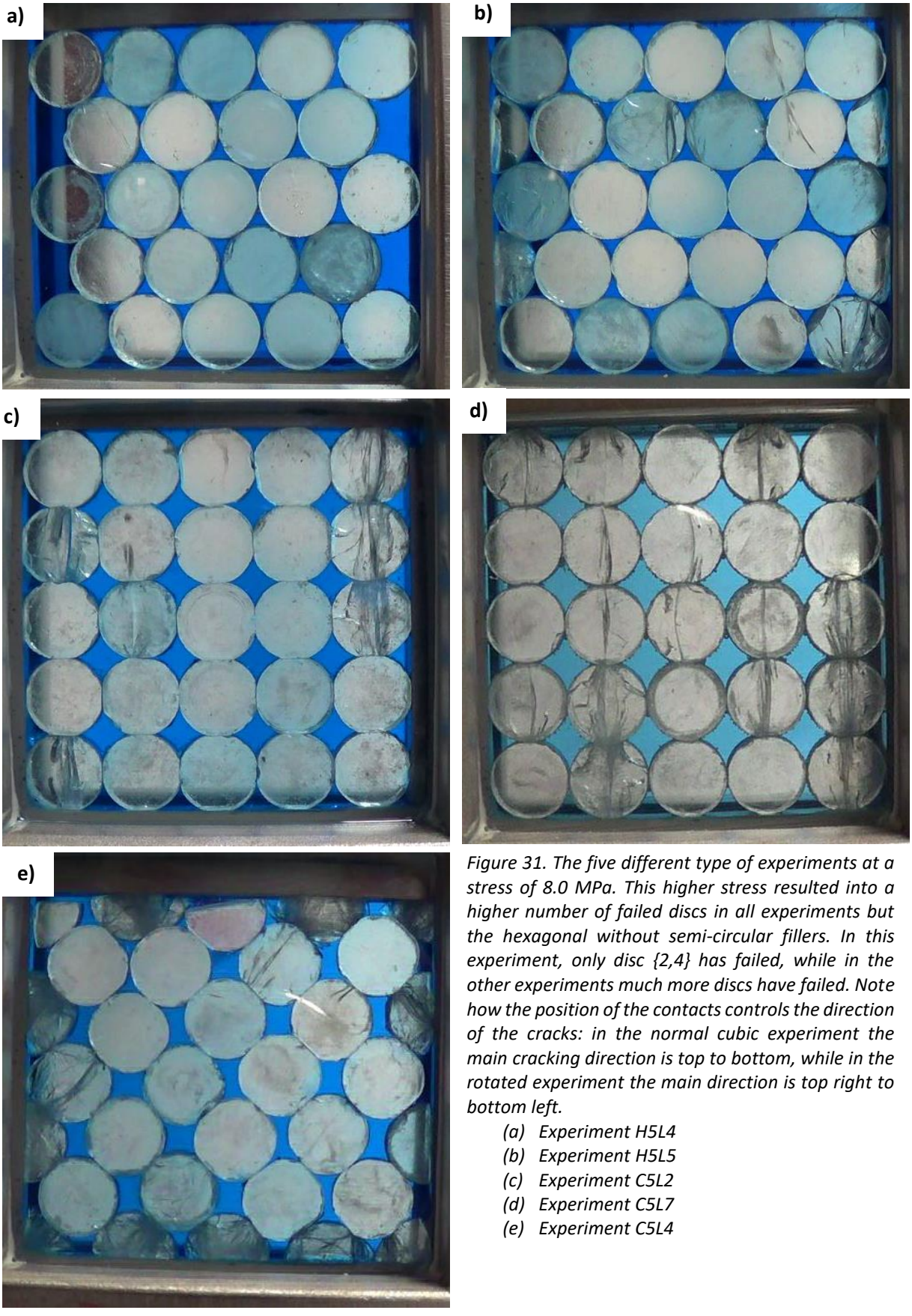

Figure 31. The five different type of experiments at a stress of 8.0 MPa. This higher stress resulted into a higher number of failed discs in all experiments but the hexagonal without semi-circular fillers. In this experiment, only disc {2,4} has failed, while in the other experiments much more discs have failed. Note how the position of the contacts controls the direction of the cracks: in the normal cubic experiment the main cracking direction is top to bottom, while in the rotated experiment the main direction is top right to bottom left.

(a) Experiment H5L4
(b) Experiment H5L5
(c) Experiment C5L2
(d) Experiment C5L7
(e) Experiment C5L4

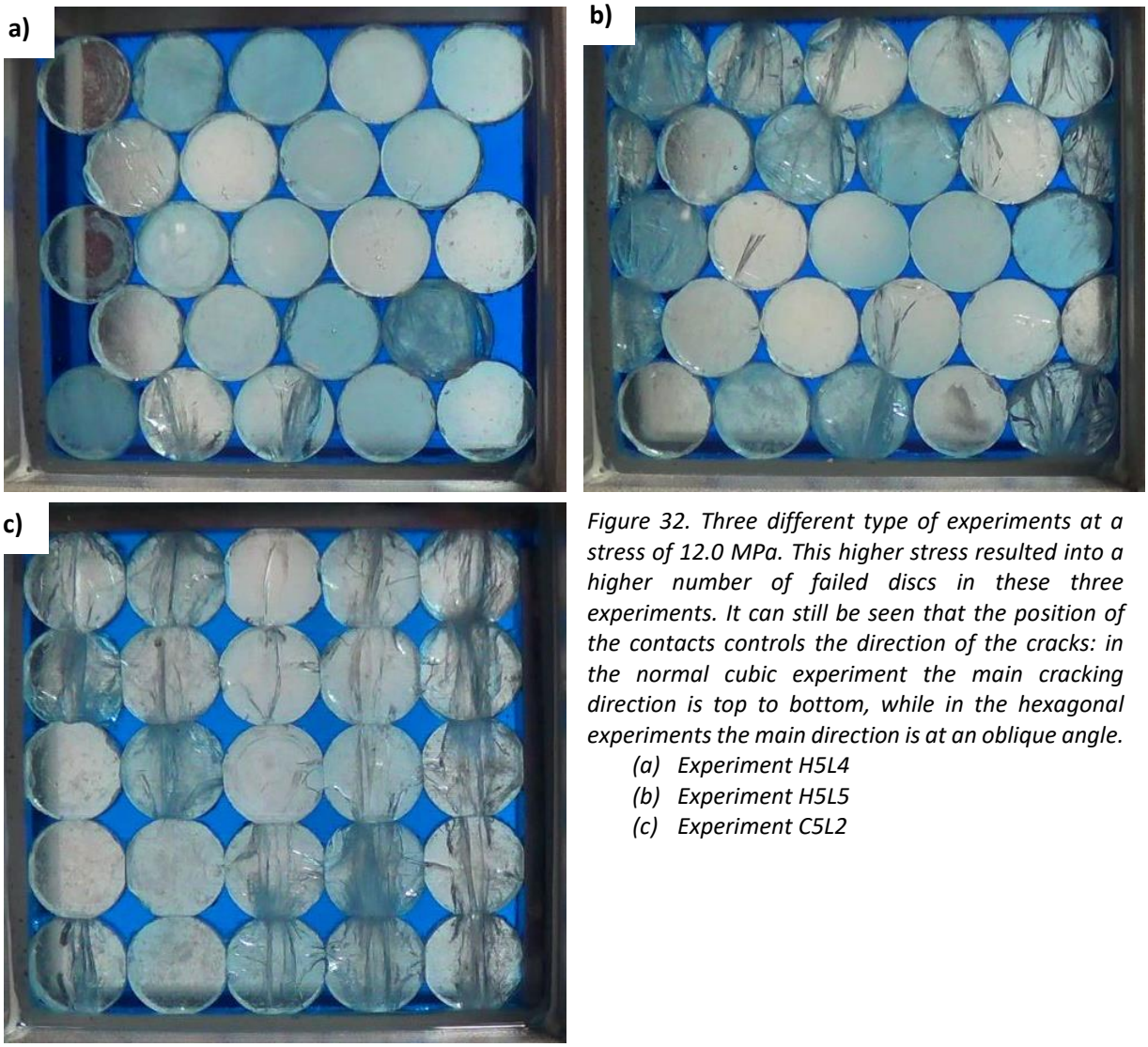

Figure 32. Three different type of experiments at a stress of 12.0 MPa. This higher stress resulted into a higher number of failed discs in these three experiments. It can still be seen that the position of the contacts controls the direction of the cracks: in the normal cubic experiment the main cracking direction is top to bottom, while in the hexagonal experiments the main direction is at an oblique angle.

(a) Experiment H5L4
(b) Experiment H5L5
(c) Experiment C5L2

whole experiment. However, despite the high stress and the higher number of failed discs, no large failure event as the one that caused the stress drop in C5L2 can be recognized.

5.1.4 Rotated cubic with flattened contacts

A first big difference can be seen in the stress-strain diagram: experiment C5L4 has much higher stress values than experiments C5L5 and C5L6. This is again caused by the hand-cut semi-circular discs: since these discs don't all have the same height, the packing is slightly off, resulting in slight height differences at the top of the pack. In C5L4, this resulted into a starting situation where the piston only touched discs {7,2} and {7,4} while in the other experiments, the piston touched disc {7,3} as well. This changed the stress distribution in the packing, increasing the overall stress in the system since the stress was exerted onto a lower number of contacts.

Another difference can be seen in the stress-strain behaviour in experiment C5L5: at a strain of 6.5% a stress drop of 3.4 MPa can be observed. This is the only experiment in which such a large stress drop can be observed. This stress drop is caused by the formation of cracks in 26 out of a total of 32 discs in the packing.

5.2 Differences between different types of experiments

5.1.1 Experiments on hexagonal packing

The addition of semi-circular filler discs caused differences in the setup. Because the filler discs prevent the discs in the second and fourth row from expanding due to opening after failure or moving towards the open spaces, the horizontal stress in the whole system is expected to be higher during these

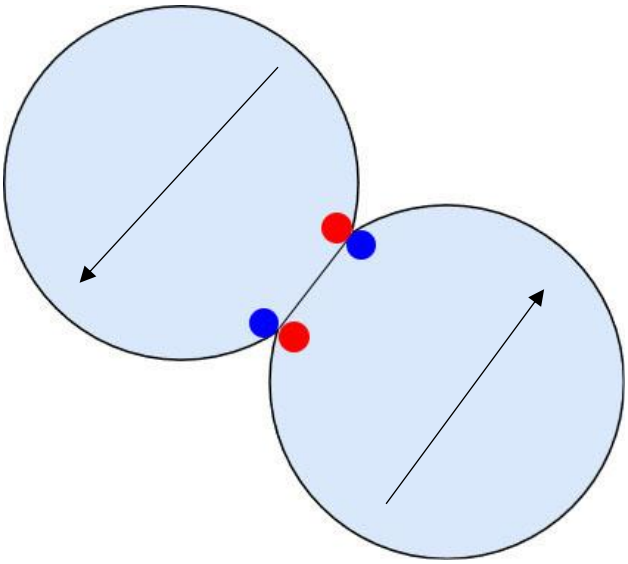

Figure 33. The positions where the cracks are most likely to form during grain boundary slip. The blue circles indicate places where cracks are least likely to form, the red circles indicate the areas where cracks are most likely to form. These colours are based on the cracks that formed in the rotated cubic experiments in the discs that experienced slip along the contact area.

experiments. This can be derived from the fact that the experiments with filer discs (H5L2, H5L5 and H5L6) had more horizontal cracks than the experiments without the filler discs. Another factor that attributed to the formation of these horizontal cracks are the semi-circular discs themselves: the presence of these discs creates an extra contact in the discs that are next to these filler discs. this changes the stress in these discs as well, resulting in an increase of stress at this contact. This increase would then result in an overall increase in stress at the left and right contacts. A third effect of the presence of the filler discs in the system can be seen in the failed discs. Without the semi-circular fillers, parts of the failed discs can easily move into the big gaps on the sides, decreasing the stress in these areas. The placement of the semi-circular discs on the sides prevents this and maintains the stress at a higher level. This can also explain the differences in the number of cracks that can be observed for the same stresses on the system (see Figures 30, 31 and 32): due to the presence of the fillers, the discs cannot move into these positions, increasing the stress at the contacts and triggering failure.

5.1.2 Experiments on cubic packing

When studying Figures 30 and 31, differences between the normal cubic experiments on flattened discs and on circular discs can be seen. At 4.0 MPa, the number of failed discs is the same: in both experiments three discs have failed. However, at 8.0 MPa a difference can be observed: the number of failed discs in experiment C5L7 is much higher than the number of failed discs in experiment C5L4. This difference can be explained by the area of the contact: since stress is a force per area, the increase in area would mean a decrease of stress on this area. A decrease of stress would then result into a lower number of failed discs, which is exactly what can be observed.

When comparing the experiments performed on flattened discs in a normal cubic or a rotated cubic setting, other differences can be observed. The direction of the cracks and the type of cracks are different. In a normal cubic system, most cracks that form are meridional cracks, accompanied by convergent cracks and some spalling cracks. The type of cracks that can be observed in the rotated cubic experiments are mainly meridional cracks as well. However, the number of convergent cracks is much lower, as well as the number of spalling cracks. In the place of the spalling cracks, vertical straight cracks can be observed. These cracks are largely influenced by grain boundary slip: due to slip of two discs along their contact area, the discs fail vertically from the side the other disc is pushed towards (see Figure 33). For example: if two discs move with a sinistral movement, it is most likely that a crack in the lower disc will form on the bottom left side of the contact, while in the top disc a crack is most likely to form at the top right position of the contact. This way, a pattern forms in the discs with consists of vertical cracks that do not continue in a straight line, but have a slight offset at every contact.

5.1.3 Differences between experiments on cubic packing and hexagonal packing

The different packing of the discs changed the recognizable features in the experiments. In contrast to the hexagonal experiments, in the normal cubic experiments all cracks that

formed were connected to either the top, the bottom or both the top and bottom contacts. Another difference between the hexagonal experiments and the normal cubic experiments is that the cubic experiments show a zone in every column where most of the deformation took place. This zone cannot be recognized in the hexagonal experiments nor in the rotated cubic experiments.

The hexagonal and rotated cubic experiments are very similar when studying the final crack distribution. Many meridional cracks can be identified that have formed between the top right and the bottom left contact, as well as straight vertical cracks between a top and bottom contact. However, the number of spalling cracks is much lower in the hexagonal experiments, and in the rotated cubic experiment, no convergent cracks can be seen accompanying the vertical straight cracks, which can be seen in the hexagonal experiments. These differences are mainly caused by the formation of these cracks: in the rotated cubic experiments, these vertical cracks have formed due to grain boundary sliding and the changes in the stress field thereof. The vertical straight cracks in the hexagonal experiments were caused by the presence of an extra contact on the side of the disc, which resulted into a larger stress field in the vertical direction.

5.3 The influence of the boundary conditions on the experiments

The two most important boundary conditions that can affect the outcome of the experiment are both caused by the setup: firstly, the difference in stiffness between the steel frame and the sugar glass can cause differences in behaviour of the discs that are in contact with the steel frame. In the discs that were in contact with the steel frame, much more deformation can be observed compared to the other discs. This is one of the reasons that the structures that are formed in these outer discs are not studied. Another reason being that these discs do not always have the correct number of contacts (for the hexagonal and the rotated cubic experiments).

Secondly, the fact that the research was done on a uniaxially deformed sample caused differences with natural samples, since sand grains can move in a horizontal direction as well as in a vertical direction and the horizontal movement of the sugar glass discs was limited by the steel frame on the side. The horizontal movement that was observed in the sugar glass experiments was caused by large deformation in some of the semi-circular discs on the edges of the aggregate, that could cause some horizontal movement. Extra horizontal movement would cause more slip along the contact surfaces, making the experiments better for research on the formation of cracks due to slip along the contact area. If the experiments were done in a triaxial setting, the horizontal expansion of the aggregate could have been controlled. This would result into experiments that would give insight on the influence of horizontal movement, and thus of grain boundary slip, on the behaviour of the system.

The small variations in stress that can be observed near the end of every experiment (Figure 9) can be explained by rotation of failed discs, the formation of new (micro)fractures in already failed grains or shearing along the failure planes. These events may release some stress, without immediate failure of the discs. This could then result into the variations in stress that are observed. Another option is that these variations may be caused by a slight asymmetry in the orientation of the piston, which then could move along the side walls of the experimental cell in a stick-slip-like pattern, and of which the magnitude of stress difference increases as the load on the piston increases. This means that the movement of the piston along the wall was measured during these events and the variabilities are small errors in the data.

5.4 Comparison to micrographs

When comparing the results of the experiments with the microscope images of deformed quartz sand aggregates, similarities and differences can be found. A major similarity is the fact that all of the major cracks have formed between two grain-to-grain contacts. The fact that multiple cracks can run between the same two contact surfaces (e.g. a meridional crack and multiple convergent cracks) can also be recognized in the micrographs (see Figure 34). However, when comparing the different packed systems, big differences can be identified between the experiments and the micrographs.

5.4.1 Differences and similarities between the normal cubic packed experiments and the micrographs

The biggest difference between the micrographs and the normal cubic experiments is the presence of a multitude of vertically orientated cracks, both meridional and convergent cracks. The orientation of these cracks is caused by the stress distribution in the discs: since the discs have contacts in the same position as the stress is applied onto the system (on the top and bottom side), the stress at these contacts will be highest. This then causes cracks between these two surfaces, which translate to meridional and convergent cracks. In the situation of a sand aggregate, the grains have contacts at random positions, but usually more contacts, creating a lower stress distribution in the grain (Omidvar et al., 2012, Figure 3) and causing a different stress distribution throughout the grain. This means that the stress can cause cracks in a more horizontal position, as can be seen in the micrographs.

A second difference is also caused by the packing of the grains or discs: in a perfect cubic packed system, every disc has four contact sides and no open spaces, other than the pores, can be found in the system. An uncompacted random packed system contains many gaps between grains, where grains are pused into when the sample is compacted. This causes a lot of horizontal stresses in the system, creating more (sub)-horizontally oriented cracks.

The above arguments show that the cubic packed sugar glass setup does not serve as a good analogue for quarz sand aggregates. This however is caused by the packing and not necessarily by the characteristics of the sugar glass.

5.4.2 Differences and similarities between the rotated cubic packed experiments and the micrographs

The structures that formed in the rotated cubic sugar glass experiments are more comparible to the structures as observed in the micrographs. The meridional and convergent cracks are at an angle with the stress direction, which can also be observed in the micrographs. However, the vertical straight cracks that are caused by grain boundary sliding are less prominent in the micrographs and it is difficult

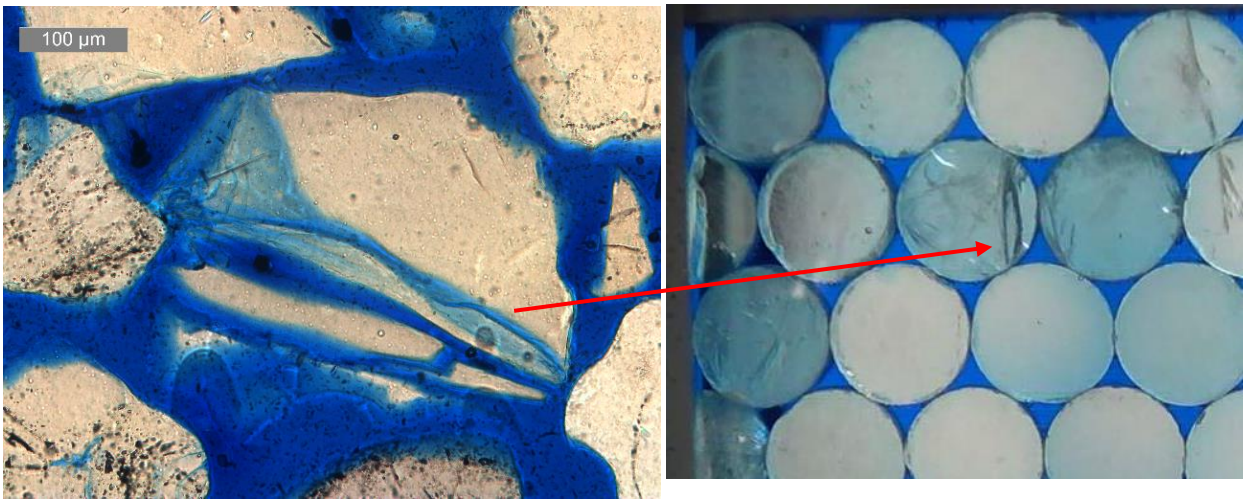

Figure 34. Similarities between structures in a deformed quartz grain (Brzesowsky et al, 2014, left) and a deformed sugar glass disc (right, experiment H5L5, close-up of Figure 13b).

to relate the vertical cracks that are present to the movement of the discs, since the motion of the grains cannot be studied directly.

5.4.3 Differences and similarities between the hexagonal packed experiments and the micrographs

Hexagonal packing is more similar to random packed systems, caused by the higher amount of contacts per disc. However, there still are some differences. Without the use of semi-circular filler discs, a compressed system experiences less horizontal stress. This is caused by the open gaps on the sides, which cause a higher mobility of the discs in the second and fourth row. These discs can partially move into these pores or when failed parts can break off fo it and move toward these pores, lowering the horizontal stresses in the system and preventing the formation of more horizontally-oriented cracks.

The addition of the semi-circular fillers counteract this horizontal movement of the discs in the second and fourth row, which causes an increase in horizontal stresses, creating more horizontal cracks. This can best be noted in experiments where the packing of the discs was not perfect so that grains didn't fit in neat rows (best example is experiments H5L6). Here the discs first had to be pushed into the open gaps, which caused the horizontal stress to rise and horizontal cracks would form between the left and the right contacts (Figure 18c). This way of packing comes closes to the random packing. The structures that can be found in the sugar glass experiments are similar to the ones that can be found in the micrographs. This means that the sugar glass experiments can be used as a analogue for structures forming in quartz sand. However, the stress necessary to form these structures is lower during the sugar glass experiments. This means that the experimetns can be used to study the structures that form in sugar glass, but cannot be used to study at what stress quartz grains fail.

5.5 Comparison with the existing literature

The brittle behaviour of sugar glass discs has previously been studied by Dik et al (2016). He performed his experiments on three-layers systems, both hexagonal and cubic. The biggest differences between his experiments and the ones described above is the influence of the boundaries on the experiment: two out of the three layers of Dik et al. (2016) were in contact with the steel frame or the steel piston while with the experiments described above two out of five contacts consist of a steel-sugar glass contact. The differences in stiffness between two contacts can cause a different behaviour in the material, causing a higher crack density in these discs. These differences could also affect the only layer that wasn't in contact with steel, since the cracks that formed in the top or bottom layer could have continued through to this second layer. The addition of two extra layers minimize the effect of these boundary conditions in the inner discs.

When comparing the results of the hexagonal experiments performed by Dik et al (2016) and the experiments performed on hexagonal packing without the semi-circular filler discs, which can be found in this research (H5L1, H5L3 and H5L4), it can be noted that the effect of the difference in stiffness between the steel and the sugar glass can be seen in both cases. The discs along the top and bottom boundary are all heavily deformed. However, the biggest differences can be found in the layers between these boundary layers. In the experiments performed by Dik et al., two discs in the middle row were heavily deformed, one was slightly deformed, and the other disc remained visibly undeformed.

5.5 Further research

In order to expand on this research, new experiments can be performed on sugar glass in order to compare the structures to quartz sand:

- The effect of different lengths of contact surface on the type and initiation of cracks
- The roughness of the contact surface on the type and initiation of cracks
- The influence of contact areas on the hexagonal experiments
- The behaviour of the sugar glass in a triaxial system, or with compressible sides (e.g. a piece of rubber allowing the aggregate to expand horizontally)

6. Conclusion

In order to study the structures that form in compacted sand aggregates, sugar glass discs can be used as analogue. The cracks that form from contact to contact can be subdivided into straight, meridional, convergent or spalling cracks. In a cubic packing, vertical meridional and convergent cracks can be seen, as well as spalling cracks that have formed from either the top or bottom to one of the side contacts. Highly deformed zones can be recognized in all five rows: here most of the compaction takes place.

The experiments performed on rotated cubic packed sugar glass with flattened contact sides provided insight in the formation of cracks during grain boundary sliding: the pattern of cracks is the same in every experiment, showing vertical cracks initiating at the edges of the contacts, breaking off the sides of the discs.

The results of the hexagonal experiments were slightly different: the type of cracks were different since the distribution and the number of contacts along the rims of the discs was different. This resulted in an overall decrease of stress in the system and an increase of resistance against the stress. The cracks that formed in the hexagonal and rotated cubic experiments were more similar to the cracks observed in micrographs of compressed sand aggregates. The micrographs showed that most of the cracks formed at an oblique angle to the compressional direction (even though exact angles are non-relevant, since the cracks are 3D structures that are viewed in a 2D cross section). This means that the sugar glass can serve as an analogue for quartz sand when studying the patterns that form within the quartz sand grains. Since the sugar glass samples showed more deformation features at a lower maximum stress than the quartz sand aggregates showed at higher maximum stress, the amount of stress in the sugar glass samples cannot directly be related to the amount of stress expected in quartz sand.

Acknowledgments

My grattitude goes towards Chris Spiers for the idea of this project and to Suzanne Hangx for the help she provided during the project. I would also like to thank Colin Peach for helping me work with the Instron and Floris van Oort and Gert Kastelein for making the necessary equipment with which the project could be executed.

References

Brzesowsky, R. H.; Hangx, S. J. T.; Brantut, N.; Spiers, C. J., Compaction creep of sands due to time-dependent grain failure: Effects of chemical environment, applied stress, and grain size. J. Geophys. Res. 2014, 119, (10), 7521-7541.

Brzesowsky, R. H.; Spiers, C. J.; Peach, C. J.; Hangx, S. J. T., Failure behavior of single sand grains: Theory versus experiment. J. Geophys. Res. 2011, 116, (B6), B06205.

Brzesowsky, R. H.; Spiers, C. J.; Peach, C. J.; Hangx, S. J. T., Time-independent compaction behavior of quartz sands. J. Geophys. Res. 2014, 2013JB010444.

Brzesowsky, R.H.; Micromechanics of sand grain failure and sand compaction. Geologica Ultraiectina 1995; no. 133

Ehrenberg, S. N., & Nadeau, P. H. (2005). Sandstone vs. carbonate petroleum reservoirs: A global perspective on porosity-depth and porosity-permeability relationships. AAPG bulletin, 89(4), 435-445.

Guéguen, Y., & Fortin, J. (2013). Elastic envelopes of porous sandstones. *Geophysical Research Letters*, *40*(14), 3550-3555.

Hangx, S. J. T.; Spiers, C. J.; Peach, C. J., Creep of simulated reservoir sands and coupled chemical-mechanical effects of CO2 injection. J. Geophys. Res. 2010, 115, B09205.

Heap, M. J., Brantut, N., Baud, P., & Meredith, P. G. (2015). Time-dependent compaction band formation in sandstone. Journal of Geophysical Research: Solid Earth, 120(7), 4808-4830.

Hiramatsu, Y., and Y. Oka (1966), Determination of the tensile strength of rock by a compression test of an irregular test piece, Int. J. Mech. Min. Sci. Geomech. Abstr., 3(2), 89–90, doi:10.1016/0148-9062(66)90002-7.

Jäger, J., Uniaxial deformation of a random packing of particles. Archive of Applied Mechanics 1999, 69, (3), 181-203.

Marketos, G., & Bolton, M. D. (2010). Flat boundaries and their effect on sand testing. International Journal for numerical and analytical methods in geomechanics, 34(8), 821-837.

Nguyen, V. H., Gland, N., Dautriat, J., David, C., Wassermann, J., & Guelard, J. (2014). Compaction, permeability evolution and stress path effects in unconsolidated sand and weakly consolidated sandstone. International Journal of Rock Mechanics and Mining Sciences, 67, 226-239.

Omidvar, M.; Iskander, M.; Bless, S., Stress-strain behavior of sand at high strain rates. International Journal of Impact Engineering 2012, 49, 192-213.

Wong, T. F., & Baud, P. (1999). Mechanical compaction of porous sandstone. Oil & Gas Science and Technology, 54(6), 715-727.

Wong, T.-f.; Baud, P., The brittle-ductile transition in porous rock: A review. J. Struct. Geol. 2012, 44, (0), 25-53.

Zhang, J.; Wong, T.-F.; Davis, D. M., Micromechanics of pressure-induced grain crushing in porous rocks. J. Geophys. Res. 1990, 95, (B1), 341-352.